

CAPITAL UNIVERSITY OF SCIENCE AND
TECHNOLOGY, ISLAMABAD



**MHD Tangent Hyperbolic
Nanofluid Past a Stretching Sheet
with the Effect of Joule Heating
and Chemical Reaction**

by

Maria Qamar

A thesis submitted in partial fulfillment for the
degree of Master of Philosophy

in the

Faculty of Computing

Department of Mathematics

2019

Copyright © 2019 by Maria Qamar

All rights reserved. No part of this thesis may be reproduced, distributed, or transmitted in any form or by any means, including photocopying, recording, or other electronic or mechanical methods, by any information storage and retrieval system without the prior written permission of the author.

To my parents, my late husband, my beloved daughter, my brother and sisters.



CERTIFICATE OF APPROVAL

MHD Tangent Hyperbolic Nanofluid Past a Stretching Sheet with the Effect of Joule Heating and Chemical Reaction

by

Maria Qamar

(MMT153009)

THESIS EXAMINING COMMITTEE

S. No.	Examiner	Name	Organization
(a)	External Examiner	Dr. Tanveer Akbar Kiani	COMSATS, Islamabad
(b)	Internal Examiner	Dr. Muhammad Afzal	CUST, Islamabad
(c)	Supervisor	Dr. Shafqat Hussain	CUST, Islamabad

Dr. Shafqat Hussain

Thesis Supervisor

April, 2019

Dr. Muhammad Sagheer

Head

Dept. of Mathematics

April, 2019

Dr. Muhammad Abdul Qadir

Dean

Faculty of Computing

April, 2019

Author's Declaration

I, **Maria Qamar** hereby state that my M.Phil thesis titled “**MHD Tangent Hyperbolic Nanofluid Past a Stretching Sheet with the Effect of Joule Heating and Chemical Reaction**” is my own work and has not been submitted previously by me for taking any degree from Capital University of Science and Technology, Islamabad or anywhere else in the country/abroad.

At any time if my statement is found to be incorrect even after my graduation, the University has the right to withdraw my M.Phil Degree.

(**Maria Qamar**)

Registration No: MMT153009

Plagiarism Undertaking

I solemnly declare that research work presented in this thesis titled “*MHD Tangent Hyperbolic Nanofluid Past a Stretching Sheet with the Effect of Joule Heating and Chemical Reaction*” is solely my research work with no significant contribution from any other person. Small contribution/help wherever taken has been dully acknowledged and that complete thesis has been written by me.

I understand the zero tolerance policy of the HEC and Capital University of Science and Technology towards plagiarism. Therefore, I as an author of the above titled thesis declare that no portion of my thesis has been plagiarized and any material used as reference is properly referred/cited.

I undertake that if I am found guilty of any formal plagiarism in the above titled thesis even after award of M.Phil Degree, the University reserves the right to withdraw/revoke my M.Phil degree and that HEC and the University have the right to publish my name on the HEC/University website on which names of students are placed who submitted plagiarized work.

(Maria Qamar)

Registration No: MMT153009

Acknowledgements

All of the appreciations are for **ALLAH** who is most ever lasting and the sustainer of this universe. Everything belong to him whatever in the heavens and whatever on the earth. Countless respect and endurance for **Prophet Muhammad (Peace be upon him)**, the fortune of knowledge, who took the humanity out of ignorance and shows the rights path. I would first like to thank my supervisor **Dr. Shafqat Hussain**, Associate Professor, Capital University of Science and Technology, Islamabad who suggested the problem. The doors towards supervisor were always open whenever I ran into a trouble spot or had a question about my research or writing. He consistently allowed this paper to be my own work, but steered me in the right the direction whenever he thought I needed it. I deem it as my privilege to work under his able guidance. Also special thanks to my teacher **Dr. Muhammad Sagheer** and all faculty memebers.

(Maria Qamar)

Registration No: MMT153009

Abstract

The main objective of this dissertation is to focus on a numerical study of magnetohydrodynamic (MHD) tangent hyperbolic nanofluid past a stretching sheet with convective boundary condition. Impact of joule heating and chemical reaction has also been incorporated. A mathematical model which resembles the physical flow problem has been developed. Similarity transformations are used to convert partial differential equations (PDEs) into a system of nonlinear ordinary differential equations (ODEs). The resulting system of ordinary differential equations (ODEs) is solved numerically by using shooting method and obtained numerical results are compared with Matlab bvp4c built in function, which shows an excellent agreement. Effects of various physical parameters on the dimensionless velocity, temperature, and concentration profiles are shown in the form of graphs. Numerical values of skin friction coefficient, Nusselt number (heat transfer rate), and Sherwood number (mass transfer rate) are also computed. The effects of different physical parameters on the flow and heat transfer characteristics are discussed in detail.

Contents

Author's Declaration	iv
Plagiarism Undertaking	v
Acknowledgements	vi
Abstract	vii
List of Figures	x
List of Tables	xi
Abbreviations	xii
Symbols	xiii
1 Introduction	1
2 Basic Terminologies and Governing Equations	6
2.1 Fluid Flows	6
2.2 Types of Fluid	7
2.3 Types of Flow	8
2.4 Some Basic Definitions of Heat Transfer	10
2.5 Thermal Conductivity and Diffusivity	11
2.6 Dimensionless Numbers	12
2.7 Fundamental Equations of Flow	14
2.8 Solution Methodology	16
3 MHD Tangent Hyperbolic Nanofluid with Convective Boundary Condition	19
3.1 Problem Formulation	19
3.2 Similarity Transformation	22
3.3 Physical Quantities of Interest	27
3.4 Numerical Technique	29
3.5 Result and Discussion	30

4	Impact of Chemical Reaction and Joule Heating on MHD Nanofluid	40
4.1	Mathematical Modeling	40
4.2	Similarity Transformation	41
4.2.1	Physical Quantities of Interest	42
4.3	Numerical Solution	43
4.4	Result and Discussion	45
5	Conclusion	56
	Bibliography	57

List of Figures

3.1	Schematic diagram of physical model.	20
3.2	Effect of n on $f'(\eta)$	33
3.3	Effect of n on $\theta(\eta)$	33
3.4	Effect of n on $\phi(\eta)$	34
3.5	Effect of We on $f'(\eta)$	34
3.6	Effect of Bi on $\theta(\eta)$	35
3.7	Effect of γ on $f'(\eta)$	35
3.8	Effect of γ on $\theta(\eta)$	36
3.9	Effect of γ on $\phi(\eta)$	36
3.10	Effect of δ on $f'(\eta)$	37
3.11	Effect of δ on $\theta(\eta)$	37
3.12	Effect of δ on $\phi(\eta)$	38
3.13	Effect of Nr on $\theta(\eta)$	38
3.14	Effect of Bi on $\theta(\eta)$	39
3.15	Effect of Pr on $\theta(\eta)$	39
4.1	Effect of M on $f'(\eta)$	49
4.2	Effect of M on $\theta(\eta)$	49
4.3	Effect of n on $f'(\eta)$	50
4.4	Effect of n on $\theta(\eta)$	50
4.5	Effect of We on $\theta(\eta)$	51
4.6	Effect of Pr on $\theta(\eta)$	51
4.7	Effect of Pr on $\phi(\eta)$	52
4.8	Effect of Nt on $\theta(\eta)$	52
4.9	Effect of Nt on $\phi(\eta)$	53
4.10	Effect of Nr on $\theta(\eta)$	53
4.11	Effect of Nr on $\phi(\eta)$	54
4.12	Effect of Bi on $\theta(\eta)$	54
4.13	Effect of Bi on $\phi(\eta)$	55
4.14	Effect of ϵ on $\theta(\eta)$	55

List of Tables

3.1	Numerical results of skin friction for increasing values of M with $We = \delta = n = \gamma = 0$	31
3.2	Numerical results of skin friction $-f''(0)$ for gradually increasing values of physical parameters.	32
4.1	numerical results of skin friction $-f''(0)$ and Nusselt number $-\theta'(0)$ for distinct values of Ec, Sc, Nb and Nt	46

Abbreviations

MHD	Magneto-hydrodynamic
PDEs	Partial differential equations
ODEs	Ordinary differential equations
RK	Runge-Kutta

Symbols

μ	Viscosity
ν	Kinematic viscosity
τ	Stress tensor
κ	Thermal conductivity
α	Thermal diffusivity
τ_w	Wall shear stress
η	Dimensionless similarity variable
θ	Dimensionless temperature
δ	Second order slip parameter
γ	First order slip parameter
ϵ	Thermal conductivity parameter
C_p	Specific heat
Re	Reynolds number
Pr	Prandtl number
Nu_x	Nusselt number
Sh_x	Sherwood number
Sc	Schmidt number
Ec	Eckert number
C_f	Skin friction coefficient
T	Temperature
T_∞	Free stream temperature
T_w	Wall temperature
U_∞	Free stream velocity

Chapter 1

Introduction

The layer in which viscous effects are more significant is named as boundary layer around which the fluid is flowing. In 1904 Ludwing Prandtl at third international conference in Germany presented the idea of boundary layer. Boundary layer is universal in a number of natural flows and now a days concept of fluid flow using in engineering applications, such as extrusion of plastic, glass blowing, the earth's atmosphere, ship and air vehicles etc [1]. A fluid flow problem related to boundary layer approximation considered along the stretching sheet was first discussed by Skiadis [2]. The flow past a stretching surface was examined by Crane [3]. Dandapat and Gupta [4] analyzed the heat transfer flow in a viscoelastic fluid along a stretching sheet. It was concluded that temperature profile is decreased by increasing the values of the Prandtl number. Over a continuous solid surface, the behaviour of boundary layer was analyzed in detail and compared it with moving surface of finite length. Fluid flow has various types of states for example, uniform or non-uniform, compressible or incompressible, rotational or irrotational, steady or unsteady, viscous or inviscid etc, Genick [5]. Study of fluid flow over a stretching surface has great importance in engineering applications, electronic devices, metal spinning, extrusion etc. Fluid flow passing through stretching sheet is a phenomenon of keen interest for many researchers, for example it includes the study of Zheng *et al.* [6], Gireesha *et al.* [7] and Shehzad *et al.* [8] due to its wide application as described above.

The study of magnetic properties for electrically conducting fluids is called magneto-hydrodynamics (MHD). The idea of MHD fluid flow was first introduced by Physicist, Alfven [9]. Rashidi *et al.* [10] ascertained the MHD flow of nanofluid over a stretching sheet with impact of thermal radiation. They reported that temperature profile increases with the impact of nanoparticles present in the base fluid. Magneto-hydrodynamic has a lot of applications in different fields of engineering like cooling of reactors, design for heat exchangers, a power generator and MHD accelerator as discussed by Hari *et al.* [11]. Zhang *et al.* [12] investigated the MHD flow and radiation heat transfer of nanofluids with chemical reaction and variable surface heat flux. They concluded that radiations and magnetic field have significant impact on velocity field, for increasing values of magnetic field fluid, the velocity decreases. Ibrahim and Suneetha [13] investigated the impact of Joule heating and also explained about viscous dissipation on MHD convective flow over a surface considering the effect of radiation. By investigating the magneto-micropolar nanofluids under the effect of variable thermal diffusivity, Bilal *et al.* [14] concluded that for increasing values of permeability parameter, velocity components like angular velocity and velocity distribution over a stretching surface including stream velocity were all enhanced. Hayat *et al.* [15] explored the impact of chemical reaction in magneto-hydrodynamic flow through a nonlinear radially stretching surface. They analyzed that the Nusselt number is an increasing function of power-law index. Atif *et al.* [16] explored the idea of magneto-hydrodynamic micropolar Carreau nanofluid having the properties of induced magnetic field and concluded that thermal profile increases for enhancing values of the Brownian motion parameter.

A liquid containing nanometer-sized particles is called nanofluid. These particles are termed as nanoparticles ranges between 1 to 100 nanometer in size. To enhance the base fluid's thermal conductivity like ethylene glycol, water, propylene glycol etc, nanofluids are used. Choi and Eastman [17] introduced the idea of improving the thermal conductivity by including the nanoparticles. Choi *et al.* [18] investigated that thermal conductivity of heat transfer fluids enhanced by addition of small amount of nanoparticles. Nanoparticles are typically made

of carbides (SiC), nonmetals (carbon nanotubes), metals (Al, Cu) and the base fluid is usually taken as water, ethylene glycol etc. [19]. Izadi *et al.* [20] numerically investigated the laminar forced convective flow of nanofluid in an annulus. They have many biomedical and engineering applications, e.g., in cancer therapy, process industries, nuclear reactors, microelectronics as discussed by Wong *et al.* [21]. Nayak *et al.* [22] investigated the magneto-hydrodynamic flow of nanofluids through a stretching sheet including the impact of thermal radiation. In their study, it was reported that the velocity field is enhanced for increasing values of the buoyancy parameter.

In the last few decades, many researchers paid their attention to non-Newtonian fluid because of its wider applications. Tangent hyperbolic fluid is one of the most important categories of non-Newtonian fluid, that has ability to characterise the shear thinning behaviour Kumar *et al.* [23]. Materials including whipped cream, ketchup, paints and lava [24] are some example of this type of fluid. Rehman *et al.* [25] scrutinized the combined effects of thermal radiation and stratification of tangent hyperbolic fluid and reported that the temperature of tangent hyperbolic fluid is enhanced for increasing values of thermal radiation parameter. Shafiq *et al.* [26] explored the bioconvective magneto-hydrodynamic fluid flow of tangent hyperbolic fluid including microorganism under the effect of magnetic field and concluded that for increasing values of thermophoresis parameter energy distribution also increases. Salahuddin *et al.* [1] investigated the tangent hyperbolic nanofluid considering the stagnation point taken along stretching cylinder and reported that for greater values of the Lewis number show increasing behaviour of Sherwood number. Naseer *et al.* [27] explored the idea of tangent hyperbolic fluid for momentum boundary layer flow through a stretching cylinder. In their study, it was noted as values of prandtl number increased temperature field also increased. Impact of Lorentz forces on tangent hyperbolic fluid flow past a stretching sheet was examined by Prabhakar *et al.* [28]. They reported that for increasing values of Brownian motion parameter a decrement is shown in the concentration of nanoparticles.

Kandasamy *et al.* [29] explored the combined effects of heat transfer rate and chemical reaction over a wedge with suction or injection. It was observed that the flow field is highly influenced by chemical reaction, suction and heat source at the wall of the wedge. Alam *et al.* [30] studied the combined effects of thermophoresis and chemical reaction on heat transfer and mixed convective mass flow along an inclined plate including the impact of Joule heating and additional effect of viscous dissipation. They concluded that mass flux of particle is as small as the stream velocity and temperature profile are not influenced by thermophysical phenomenon experienced by relatively small number of particles. Abbas *et al.* [31] investigated the analytical solution of binary chemical reaction considering the stagnation point flow for Casson fluid with thermal effect. Some further studies related to chemical reactions have been discussed in Refs. [32, 33].

The demonstration of this thesis is to explore the mathematical results of magneto-hydrodynamic fluid flow of hyperbolic fluid through a stretched layer including convective boundary conditions. The set of non-linear partial differential equations (PDEs) are converted into a set of governing ordinary differential equations (ODEs) by use of applicable transformation called similarity transformation. Using MATLAB function `bvp4c` and the shooting technique various numerical results are validated. Further impact of different parameters are discussed through graphs and tables in detail.

Layout of Thesis

This dissertation is further composed of the following chapters.

Chapter 2 includes some basic definitions and physical parameters which are useful for upcoming work and discusses the numerical technique which will be used to solve the dominant equations.

Chapter 3 provides the review work of research paper of Ibrahim [34] in which the study has been carried out for magneto-hydrodynamic flow of hyperbolic fluid over

a stretching sheet including slip conditions. The `bvp4c` code which is MATLAB built-in function has been used for computing the solution of nonlinear ODEs. Numerical results for various parameters are compiled through tables and graphs.

Chapter 4 extends the work of [34] for the impact of chemical reaction and Joule heating. By utilizing similarity transformation we transform the set of governing nonlinear PDEs into the nonlinear ODEs. Results for various parameters are discussed through graphs and tables.

Chapter 5 summarizes the whole study with concluding remarks.

Chapter 2

Basic Terminologies and Governing Equations

In this chapter, some basic definitions, laws and dimensionless numbers are explained, which will be helpful in continuing the work for the next chapters. References which are used for definitions are: [5, 35–40]

2.1 Fluid Flows

Definition 2.1. (Fluid)

“A fluid is a substance that deforms continuously under the application of a shear (tangential) stress no matter how small the shear stress may be.”

Definition 2.2. (Fluid Mechanics)

“Fluid mechanics is that branch of science which deals with the behaviours of the fluids (liquids or gasses) at rest or in motion.

Fluid mechanics further divided into two types:

1. Fluid Static
2. Fluid Dynamics”

Definition 2.3. (Fluid Statics)

“Fluid statics is a branch of fluid mechanics that deals with the fluid and its properties at constant position is known as fluid statics.”

Definition 2.4. (Fluid Dynamics)

“The branch of mechanics that deals with the characteristics of fluid in state of progression from one place to another place is known as fluid dynamics.”

Definition 2.5. (Viscosity)

“There is a property that represents the internal resistance of a fluid to motion or the fluidity, and that property is the viscosity. The force a flowing fluid exert on a body is called drag force and the magnitude of this force depends, in part, on viscosity.”

Mathematically,

$$\text{viscosity}(\mu) = \frac{\text{shear stress}}{\text{shear strain}}. \quad (2.1)$$

Definition 2.6. (Kinematic Viscosity)

“It is defined as the ratio between the dynamic viscosity and density of fluid. It is denoted by Greek symbol ν called ‘nu’.

Mathematically,

$$\nu = \frac{\mu}{\rho}. \quad (2.2)$$

The dimension of kinematic viscosity is given as: $[L^2T^{-1}]$.”

2.2 Types of Fluid

Definition 2.7. (Ideal fluid)

“A fluid, which is incompressible and is having no viscosity, is known as an ideal fluid. ideal fluid is only an imaginary fluid as all the fluid, which exist, have some viscosity.”

Definition 2.8. (Real fluid)

“A fluid, which possesses viscosity, is known as real fluid. In actual practice, all the fluids, are real fluids.”

Definition 2.9. (Newtonian fluid)

“A real fluid, in which the shear stress is directly, proportional to the rate of shear strain(or velocity gradient), is known as a Newtonian fluid.”

Definition 2.10. (Non-Newtonian fluid)

“A real fluid, in which the shear stress is not proportional to the rate of shear strain(or velocity gradient), is known as a non-Newtonian fluid.” Mathematically, it can be expressed as:

$$\tau_{xy} \propto \left(\frac{du}{dy} \right)^m, \quad m \neq 1$$

$$\tau_{yx} = \mu \left(\frac{du}{dy} \right)^m, \quad (2.3)$$

there are some examples of non-Newtonian fluid:

Maxwell fluid, Tangent hyperbolic fluid, Micropolar fluid etc.

Definition 2.11. (Flow)

“Flow is defined as, the deformation of material under the effect of different forces. As deformation increases continuously without limitations that process is called flow.”

2.3 Types of Flow

Definition 2.12. (Laminar Flow)

“The highly ordered fluid motion characterized by smooth layers of fluid is laminar. The word laminar comes from the movement of adjacent fluid particles together in laminates. The flow of high-viscosity fluid such as oils at low velocities is typically laminar flow.”

Definition 2.13. (Turbulent Flow)

“The highly disordered fluid motion that typically occurs at high velocities and is characterized by velocity fluctuations is called turbulent flow. The flow of low-viscosity fluid such as air at high velocity is typically turbulent.”

Definition 2.14. (Compressible Flow)

“Compressible flow are one in which level of variation in density is negligible. Flow of gasses is one of the best example.” Mathematically,

$$\rho(x, y, z, t) \neq k, \quad k \text{ is constant}$$

Definition 2.15. (Incompressible Flow)

“A flow is said to be incompressible if the density remains nearly constant throughout. Therefore, the volume of every portion of fluid remain unchanged over the course of its motion when the flow is incompressible.” Mathematically,

$$\rho(x, y, z, t) = k, \quad k \text{ is constant}$$

Definition 2.16. (Internal Flow)

“If the fluid is completely bounded by a solid surfaces that flow is called internal flow. The flow in a pipe or duct is an example of internal flow. Internal flows are dominated by the influence of viscosity throughout the flow field.”

Definition 2.17. (External Flow)

“The flow of an unbounded fluid over a surface such as plate, a wire or a pipe is an external flow. In external flow the viscous effects are limited to boundary layer near solid surfaces.”

Definition 2.18. (Steady Flow)

“A steady flow is one, in which properties of the fluid are independent of time.” Mathematically,

$$\frac{d\chi}{dt} = 0,$$

where property of fluid is denoted by χ .

Definition 2.19. (Unsteady Flow)

“A fluid flow in which fluid properties are dependent of time is known as unsteady flow.” Mathematically, it can be written as

$$\frac{d\chi}{dt} \neq 0,$$

where property of fluid is denoted by χ .

2.4 Some Basic Definitions of Heat Transfer

Definition 2.20. (Conduction)

“In a thermal system heat conduction manifests itself as a thermal field. The thermal field can be steady or unsteady, linear or non-linear, with inner source or without them, with moveable or stationary borders, with basic, composed or combined boundary conditions or with phase conversion. Biot number is one of the example of conduction number.”

Definition 2.21. (Convection)

“The mechanism in which fluid is forced by external processes and when thermal energy expands in gravitational fields by the interaction of buoyancy forces is called convection. In other words, convection is the process in which heat transfer occurs due to the motion of molecules within the fluid such as air, water etc. The convection phenomena take place through diffusion or advection.” Mathematically, it is expressed as

$$q = hA(T_s - T_\infty)$$

where h indicates the rate of heat transfer coefficient, A indicates the relevant area, T_s indicates temperature at the surface and T_∞ shows the temperature away from the surface. It is divided in to following three categories further which are given as,

Definition 2.22. (Force Convection)

“Forced convection is characterized by a flow with mutual action of inertia and viscous forces. The Reynolds number, Nusselt and Prandtal are some basic characteristics of forced convection.”

Definition 2.23. (Natural Convection)

“In natural convection, the dimensionless quantities express the spontaneous heat flow in fluid or gasses due to the thermal difference caused by the difference of fluid

density. Natural convection occurs in a atmosphere in ocean and near the surface of heated or cooled bodies for example, Archimedes and Schwarzschild number are characteristics.”

Definition 2.24. (Mixed Convection)

“A flow mechanism which is simultaneously contributed by both force and free convection processes and acting simultaneously. Mixed convection is always realized when small number of velocities are characterized on calling and heating of walls.”

2.5 Thermal Conductivity and Diffusivity

Definition 2.25. (Thermal Conductivity)

“It is property of a material related to its capacity to conduct the heat. Fourier law of conduction which reveals that the rate of heat transfer by conduction to temperature gradient is

$$\frac{dQ}{dt} = -kA \frac{dT}{dx}, \quad (2.4)$$

where A , $\frac{dQ}{dt}$, k , and $\frac{dT}{dx}$ represent area, thermal conductivity, temperature and the rate of heat transfer, respectively. Thermal conductivity of most liquids decreases with the increase of temperature except water. The SI unit of thermal conductivity is $\frac{Kg.m}{s^3}$ and the dimension of thermal conductivity is $[MLT^{-3}]$.”

Definition 2.26. (Thermal Diffusivity)

“The ratio of unsteady heat conduction (k) of a substance to the product of specific heat capacity (c_p) and density (ρ) is called thermal diffusivity. It quantify the ability of a substance to transfer heat rather to store it.

Mathematically, it can be written as

$$\alpha = \frac{k}{\rho c_p}$$

2.6 Dimensionless Numbers

Definition 2.27. (Biot Number)

“Biot number expresses the ratio of heat flow transferred by convection on a body surface to the heat flow transferred by conduction in a body.” Mathematically, it is represented by Bi ,

$$Bi = \frac{hL}{\lambda} \quad (2.5)$$

where h -heat transfer coefficient; L -characteristic length and λ is thermal conductivity.

Definition 2.28. (Reynolds Number)

“It is the most significant dimensionless number which is used to analyze the different flow behaviors like laminar or turbulent flow. It helps to measure the ratio between inertial force and the viscous force. Mathematically,

$$Re = \frac{\rho U^2 L}{\mu} \implies Re = \frac{LU_\infty}{\nu}, \quad (2.6)$$

here U_∞ denotes the free stream velocity, L -the characteristics length and ν is the kinematic viscosity. At low Reynolds number laminar flow arises, where viscous forces are dominant. At high Reynolds number turbulent flow arises, where inertial forces are dominant.”

Definition 2.29. (Prandtl Number)

“This number expresses the ratio of the momentum diffusivity (viscosity) to the thermal diffusivity. It characterizes the physical properties of a fluid with convective and diffusive heat transfer. It describes, for example, the phenomena connected with energy transfer in a boundary layer. It expresses the degree of similarity between velocity and diffusive thermal fields or, alternatively, between hydrodynamic and thermal boundary layer.

$$Pr = \frac{\nu}{\alpha}, \quad (2.7)$$

Where kinematic viscosity is denoted by ν and α defines the thermal diffusivity.”

Definition 2.30. (Weissenberg Number)

“The Weissenberg number is typically defined as $We = \frac{\lambda u}{L}$ where u and L are a characteristic velocity and length scale for the flow.

The Weissenberg number indicates the relative importance of fluid elasticity for a given flow problem.”

Definition 2.31. (Nusselt Number)

“It is the ratio of total heat transfer in a system to the heat transfer by conduction. It characterizes the heat transfer by convection between a fluid and environment close to it or, alternatively, the connection between the heat transfer intensity and the temperature field in a flow boundary layer.”

Nusselt number represent dimensionless thermal transference. It is represented by Nu , Mathematically,

$$Nu = \frac{\alpha L}{\lambda}, \quad (2.8)$$

where $\alpha(wm^{-2}k^{-1})$ denotes heat transfer coefficient, $L(m)$ denotes the characteristic length and $\lambda(wm^{-1}k^{-1})$ denotes the thermal conductivity.

Definition 2.32. (Thermophoresis Parameter)

“In a temperature gradient, small particles are pushed towards the lower temperature because of the asymmetry of molecular impacts.

The resulting force which drives the particles along a temperature gradient towards the lower temperature, is called thermophoretic force and the mechanism thermophoresis.”

Definition 2.33. (Eckert Number)

“It expresses the ratio of kinetic energy to a thermal energy change.”

Mathematically,

$$Ec = \frac{W_{\infty}^2}{c_p \Delta T} \quad (2.9)$$

where W_{∞} -fluid flow velocity far from body; c_p -specific heat capacity of fluid and ΔT is temperature difference.

2.7 Fundamental Equations of Flow

Definition 2.34. (Continuity Equation)

“The conservation of mass of fluid entering and leaving the control volume, the resulting mass balance is called the equation of continuity. From this law it is concluded that mass is conserved. Mathematically form is

$$\frac{\partial \rho}{\partial t} + \nabla \cdot (\rho \mathbf{U}) = 0.$$

where, \mathbf{U} is velocity of fluid.

For steady case rate of time will be constant, so continuity equation becomes

$$\nabla \cdot (\rho \mathbf{U}) = 0.$$

For the case of incompressible flow, density does not changes so continuity equation can be re-write as,

$$\nabla \cdot \mathbf{U} = 0.”$$

Definition 2.35. (Law of Conservation of Momentum)

It is based on the momentum principle, which states that,

“The net force acting on a fluid mass is equal to the change in momentum of flow per unit time in that direction. Mathematical form of this law is

$$\rho \frac{D\mathbf{U}}{Dt} = \rho \mathbf{b} + \nabla \cdot \underline{\mathbf{T}}, \quad (2.10)$$

For Navier-Stokes equation

$$\underline{\mathbf{T}} = -p\mathbf{I} + \tau, \quad (2.11)$$

where τ is a tensor and it can be written as,

$$\tau = \mu (\nabla \mathbf{U} + (\nabla \mathbf{U})^{t*}). \quad (2.12)$$

In the above equations, $\frac{D}{Dt}$ denotes material time derivative or total derivative, ρ denotes density, \mathbf{U} denotes velocity of fluid, Cauchy stress tensor represented by

T , \mathbf{b} is the body forces, p is the pressure and t^* is transpose of matrix. Matrix form of Cauchy stress tensor is

$$\tau = \begin{pmatrix} \sigma_{xx} & \tau_{xy} & \tau_{xz} \\ \tau_{xy} & \sigma_{yy} & \tau_{yz} \\ \tau_{zx} & \tau_{zy} & \sigma_{zz} \end{pmatrix}, \quad (2.13)$$

For two-dimensional flow, we have $\mathbf{U} = [u(x, y, 0), v(x, y, 0), 0]$ and thus

$$\nabla \mathbf{U} = \begin{pmatrix} \frac{\partial u}{\partial x} & \frac{\partial v}{\partial x} & 0 \\ \frac{\partial u}{\partial y} & \frac{\partial v}{\partial y} & 0 \\ 0 & 0 & 0 \end{pmatrix}, \quad (2.14)$$

$$(\nabla \mathbf{U})^{t^*} = \begin{pmatrix} \frac{\partial u}{\partial x} & \frac{\partial u}{\partial y} & 0 \\ \frac{\partial v}{\partial x} & \frac{\partial v}{\partial y} & 0 \\ 0 & 0 & 0 \end{pmatrix}. \quad (2.15)$$

Substituting Eqs. (2.14) and (2.15) into Eq. (2.12) and then in Eq. (2.11) it is found that:

$$T_{xx} = -p + 2\mu \frac{\partial u}{\partial x} \quad (2.16)$$

$$T_{xy} = \mu \left(\frac{\partial v}{\partial x} + \frac{\partial u}{\partial y} \right). \quad (2.17)$$

Using Eqs. (2.16) to (2.17) in Eq. (2.10), we get two-dimensional Navier-Stokes equation for u component.

$$\rho \frac{Du}{Dt} = \rho b_x - \frac{\partial p}{\partial x} + \mu \left(\frac{\partial^2 u}{\partial x^2} + \frac{\partial^2 u}{\partial y^2} \right) \quad (2.18)$$

Similarly, by repeating the above process for v component, we get

$$\rho \frac{Dv}{Dt} = \rho b_y - \frac{\partial p}{\partial y} + \mu \left(\frac{\partial^2 v}{\partial x^2} + \frac{\partial^2 v}{\partial y^2} \right). \quad (2.19)$$

Definition 2.36. (Law of Conservation of Energy)

The basic principle of conservation of energy is that, “Energy can neither created nor destroyed, it can be transformed from one form to another form but total amount of an isolated system remains constant i.e. energy is conserved over time. It is the fundamental law of physics which is also known as the first law of thermodynamics.

The mathematical form of energy equation in two-dimensional for fluid can be written as,

$$\left(u \frac{\partial T}{\partial x} + v \frac{\partial T}{\partial y}\right) = \alpha \left(\frac{\partial^2 T}{\partial x^2} + \frac{\partial^2 T}{\partial y^2}\right) + \frac{\mu}{\rho C_p} \Phi^* \quad (2.20)$$

where Φ^* is dissipation function.

2.8 Solution Methodology

“Shooting Method is used to solve the higher order nonlinear ordinary differential equations. To implement this technique, we first convert the higher order ODEs to the system of first order ODEs. After that we assume the missing initial conditions and the differential equations are then integrated numerically using the Runge-Kutta method as an initial value problem. The accuracy of the assumed missing initial condition is then checked by comparing the calculated values of the dependent variables at the terminal point with their given value there. If the boundary conditions are not fulfilled up to the required accuracy, with the new set of initial conditions, then they are modified by Newtons method. The process is repeated again until the required accuracy is achieved. To explain the shooting method, we consider the following general second order boundary value problem,

$$y''(x) = f(x, y, y'(x)) \quad (2.21)$$

subject to the boundary conditions

$$y(0) = 0, \quad y(L) = A. \quad (2.22)$$

[40] By denoting y by y_1 and y_1' by y_2 , Eq. (2.21) can be written in the form of following system of first order equations.

$$\left. \begin{aligned} y_1' &= y_2, & y_1(0) &= 0, \\ y_2' &= f(x, y_1, y_2), & y_1(L) &= A. \end{aligned} \right\} \quad (2.23)$$

Denote the missing initial condition by $y_2(0) = s$, to have

$$\left. \begin{aligned} y_1' &= y_2, & y_1(0) &= 0, \\ y_2' &= f(x, y_1, y_2), & y_2(0) &= s. \end{aligned} \right\} \quad (2.24)$$

Now the problem is to find s such that the solution of the IVP (2.24) satisfies the boundary condition $y(L) = A$. In other words, if the solutions of the initial value problem (2.24) are denoted by $y_1(x, s)$ and $y_2(x, s)$, one should search for that value of s which is an approximate root the equation.

$$y_1(L, s) - A = \phi(s) = 0. \quad (2.25)$$

To find an approximate root of the Eq. (2.25) by the Newtons method, the iteration formula is given by

$$s_{n+1} = s_n - \frac{\phi(s_n)}{d\phi(s_n)/ds}, \quad (2.26)$$

or,

$$s_{n+1} = s_n - \frac{y_1(L, s_n) - A}{dy_1(L, s_n)/ds}. \quad (2.27)$$

To find the derivatives of y_1 with respect of s , differentiate (2.24) with respect to s . For simplification, use the following notations

$$\frac{dy_1}{ds} = y_3, \quad \frac{dy_2}{ds} = y_4 \quad (2.28)$$

$$\left. \begin{aligned} y_3' &= y_4, & y_3(0) &= 0, \\ y_4' &= \frac{\partial f}{\partial y_1} y_3 + \frac{\partial f}{\partial y_2} y_4, & y_4(0) &= 1. \end{aligned} \right\} \quad (2.29)$$

Now, solving the IVP Eq. (2.29), the value of y_3 at L can be computed. This value is actually the derivative of y_1 with respect to s computed at L . Setting the value of $y_3(L, s)$ in Eq. (2.27), the modified value of s can be achieved. This new value of s is used to solve the Eq. (2.24) and the process is repeated until the value of s is within a described degree of accuracy.”

Chapter 3

MHD Tangent Hyperbolic Nanofluid with Convective Boundary Condition

In this chapter, we consider the MHD tangent hyperbolic nanofluid flow with free convective boundary and second order slip condition. By means of an appropriate transformation, the governing PDEs are transformed into dimensionless coupled ODEs. These dimensionless ODEs have been solved by MATLAB built-in function known as `bvp4c`. Impact of different parameters on the energy distribution, velocity distribution and concentration profile all are analyzed via tables and graphs. Basically this chapter provides the review work of the Ref. [34].

3.1 Problem Formulation

We consider incompressible, 2D, nanofluid flow with the convective boundary conditions through a stretching sheet. For the velocity taken at the surface, second order slip condition is considered. Along x -axis we take stretching sheet with stretching velocity $u_w = ax$ where the fluid flow is bounded by the region $y > 0$. The temperature provided to the stretching surface is denoted by T_f with h_f as

the heat transfer coefficient, C_w is surface concentration, C_∞ denotes the ambient concentration and T_∞ represents the ambient temperature. With the assumption that no nanoparticles flux is present on the surface, the impact of thermophoresis is incorporated along boundary condition. A magnetic field is applied normal to the stretching surface having strength B_0 as we can see in Figure 3.1 induced magnetic field is ignored with the assumptions of small values of magnetic Reynolds number.

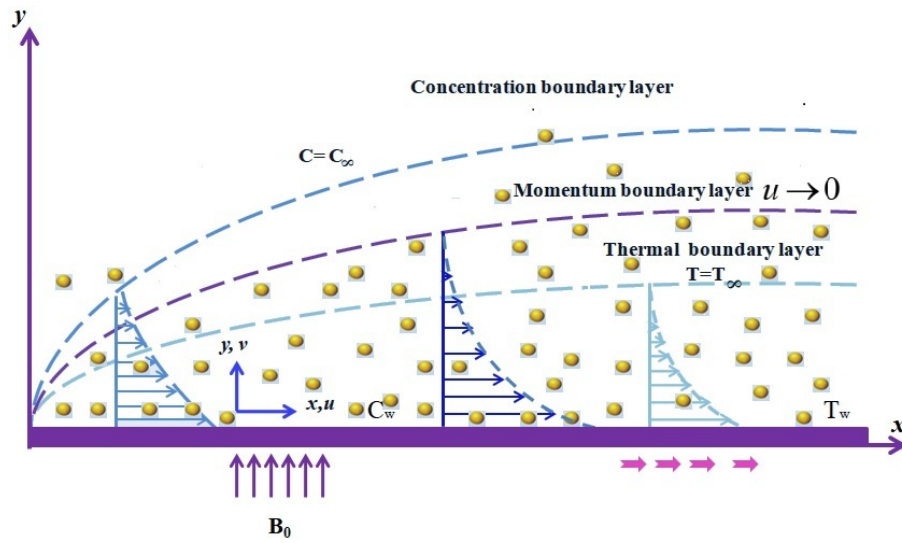


Figure 3.1: Schematic diagram of physical model.

Under the above constraints, the boundary layer equations of the tangent hyperbolic fluid with nanoparticles are given as [34]:

$$\frac{\partial u}{\partial x} + \frac{\partial v}{\partial y} = 0, \quad (3.1)$$

$$u \frac{\partial u}{\partial x} + v \frac{\partial u}{\partial y} = \nu(1-n) \frac{\partial^2 u}{\partial y^2} + \sqrt{2\nu n} \Gamma \left(\frac{\partial u}{\partial y} \right) \frac{\partial^2 u}{\partial y^2} - \frac{\sigma B_0^2 u}{\rho}, \quad (3.2)$$

$$u \frac{\partial T}{\partial x} + v \frac{\partial T}{\partial y} = \alpha \left(\frac{\partial^2 T}{\partial y^2} \right) + \Lambda \left[D_B \left(\frac{\partial C}{\partial y} \right) \left(\frac{\partial T}{\partial y} \right) + \frac{D_T}{T_\infty} \left(\frac{\partial T}{\partial y} \right)^2 \right] - \frac{1}{(\rho c_p)_f} \frac{\partial q_r}{\partial y}, \quad (3.3)$$

$$u \frac{\partial C}{\partial x} + v \frac{\partial C}{\partial y} = D_B \frac{\partial^2 C}{\partial y^2} + \frac{D_T}{T_\infty} \left(\frac{\partial^2 T}{\partial y^2} \right). \quad (3.4)$$

The related boundary conditions are as follows:

$$\left. \begin{aligned} u &= u_w + U_{slip}, & -k \frac{\partial T}{\partial y} &= h_f(T_f - T), \\ v &= 0, & D_B \frac{\partial C}{\partial y} + \frac{D_B}{T_\infty} \frac{\partial T}{\partial y} &= 0, \\ U \rightarrow U_\infty &= 0, & v &= 0, & T \rightarrow T_\infty, & C \rightarrow C_\infty & \text{as } y \rightarrow \infty, \end{aligned} \right\} \text{at } y = 0 \quad (3.5)$$

where the slip velocity at the boundary layer is denoted by U_{slip} and is defined as:

$$U_{slip} = A \frac{\partial u}{\partial y} + B \frac{\partial^2 u}{\partial y^2}. \quad (3.6)$$

Here, A and B are constants.

In the above equations, ν represents kinematics velocity, ρ is the density, ρc_p is the effective heat capacity of a nanoparticle, n stands for the power-law index, $\Lambda = \frac{\rho c_p}{\rho c_f}$ where ρc_f is fluid's heat capacity and Γ denotes time constant.

It is worth mentioning that by taking power-law index zero, problem is transformed into Newtonian fluid.

The velocity components in terms of the stream functions are given as

$$u = \frac{\partial \psi}{\partial y}, \quad v = -\frac{\partial \psi}{\partial x}. \quad (3.7)$$

In Eq. (3.3), the Rosseland approximation for heat flux q_r is given as

$$q_r = -\frac{4\sigma^*}{3\kappa^*} \frac{\partial T^4}{\partial y}. \quad (3.8)$$

Here κ^* stands for the absorption coefficient and σ^* stands for Stefan Boltzmann constant.

If temperature constant is very small, then T^4 might be expanded about T_∞ by utilizing Taylor series, given as:

$$T^4 = T_\infty^4 + \frac{4T_\infty^3}{1!}(T - T_\infty) + \frac{12T_\infty^2}{2!}(T - T_\infty)^2 + \frac{24T_\infty}{3!}(T - T_\infty)^3 + \frac{24}{4!}(T - T_\infty)^4 + \dots$$

We will ignore the higher order terms and get the form:

$$\begin{aligned}
T^4 &= T_\infty^4 + 4T_\infty^3(T - T_\infty) \\
\Rightarrow T^4 &= T_\infty^4 + 4T_\infty^3T - 4T_\infty^4 \\
\Rightarrow T^4 &= 4T_\infty^3T - 3T_\infty^4. \\
\Rightarrow \frac{\partial T^4}{\partial y} &= 4T_\infty^3 \frac{\partial T}{\partial y}. \tag{3.9}
\end{aligned}$$

Using Eq. (3.9) in Eq. (3.8) and differentiating, we have the following form:

$$\frac{\partial q_r}{\partial y} = \frac{-16\sigma^*T_\infty^3}{3k^*} \frac{\partial^2 T}{\partial y^2}. \tag{3.10}$$

3.2 Similarity Transformation

In this section the dimensional partial differential equations are converted into the non-dimensional form by means of the similarity transformation. We introduce the following dimensionless similarity variable [34]:

$$\psi = x\sqrt{av}f(\eta), \quad \eta = \sqrt{\frac{a}{\nu}}y, \quad \phi(\eta) = \frac{C - C_\infty}{C_\infty}, \quad \theta(\eta) = \frac{T - T_\infty}{T_f - T_\infty}. \tag{3.11}$$

The velocity components respectively their derivatives can be transformed as follows

- $u = \frac{\partial \psi}{\partial y} = \frac{\partial \psi}{\partial \eta} \frac{\partial \eta}{\partial y} = \sqrt{av} x f'(\eta) \sqrt{\frac{a}{\nu}} = ax f'(\eta) = a f'(\eta).$
- $\frac{\partial u}{\partial x} = \frac{\partial}{\partial x} \left(ax f'(\eta) \right) = a f'(\eta).$
- $v = -\frac{\partial \psi}{\partial x} = -\sqrt{av} f(\eta)$
- $\frac{\partial v}{\partial y} = \frac{\partial v}{\partial \eta} \frac{\partial \eta}{\partial y} = -\sqrt{av} f'(\eta) \sqrt{\frac{a}{\nu}} = -a f'(\eta).$

The continuity Eq. (3.1) is satisfied identically, that is

$$\frac{\partial u}{\partial x} + \frac{\partial v}{\partial y} = a f'(\eta) - a f'(\eta) = 0.$$

The momentum Eq. (3.2) becomes

$$\begin{aligned} a^2x(f'(\eta))^2 - a^2xf(\eta)f''(\eta) &= \nu(1-n)\frac{a^2}{\nu}xf'''(\eta) - \frac{\sigma B_0^2ax}{\rho_f}f'(\eta) \\ &+ \sqrt{2}\nu n\Gamma\sqrt{a\nu}xf''(\eta)\frac{a}{\nu}\cdot\frac{a^2x}{\nu}f'''(\eta) \end{aligned} \quad (3.12)$$

$$\begin{aligned} a^2x(f'(\eta))^2 - a^2xf(\eta)f''(\eta) &= (1-n)a^2xf'''(\eta) + a^2xnWef'''(\eta)f''(\eta) \\ &- \frac{\sigma B_0^2axf'(\eta)}{\rho_f} \end{aligned}$$

$$\begin{aligned} a^2x[(f'(\eta))^2 - f(\eta)f''(\eta)] &= a^2x[(1-n)f'''(\eta) + nWef'''(\eta)f''(\eta)] \\ &- Mf'(\eta), \end{aligned}$$

$$\Rightarrow (1-n)f'''(\eta) + f(\eta)f''(\eta) - (f'(\eta))^2 + nWef'''(\eta)f''(\eta) - Mf'(\eta) = 0$$

$$\Rightarrow (1-n)f''' + ff'' - f'^2 + nWef'''f'' - Mf' = 0. \quad (3.13)$$

Now we transform the derivatives for the temperature

- $\theta(\eta) = \frac{T - T_\infty}{T_f - T_\infty}$

$$T = T_f\theta(\eta) - T_\infty\theta(\eta) + T_\infty$$

$$\frac{\partial T}{\partial y} = \frac{\partial}{\partial y} \left(T_f\theta(\eta) - T_\infty\theta(\eta) + T_\infty \right) = T_f\theta' \sqrt{\frac{a}{\nu}} - T_\infty\theta' \sqrt{\frac{a}{\nu}}$$

$$\frac{\partial^2 T}{\partial y^2} = \frac{\partial}{\partial y} \left(T_f\theta' \sqrt{\frac{a}{\nu}} - T_\infty\theta' \sqrt{\frac{a}{\nu}} \right) = \theta'' \frac{a}{\nu} (T_f - T_\infty)$$

$$\frac{\partial q_r}{\partial y} = \frac{16\sigma^*T_\infty^3a\theta''}{3k^*\nu}$$

$$\frac{\partial C}{\partial y} = \frac{\partial}{\partial y} \left(C_\infty\phi' + C_\infty \right) = \frac{\partial C}{\partial \eta} \cdot \frac{\partial \eta}{\partial y} = C_\infty\phi' \sqrt{\frac{a}{\nu}}$$

Using the above derivatives, the left side of Eq. (3.3) gets the following form:

$$\begin{aligned} u \frac{\partial T}{\partial x} + v \frac{\partial T}{\partial y} &= -\sqrt{a\nu} f(\eta) \left[T_f \theta' \sqrt{\frac{a}{\nu}} - T_\infty \theta' \sqrt{\frac{a}{\nu}} \right] \\ &= -a T_f \theta' f(\eta) - T_\infty a \theta' f(\eta). \end{aligned} \quad (3.14)$$

To convert the right side of Eq. (3.3) into dimensionless form, we proceed as follows.

$$\begin{aligned} \alpha \frac{\partial^2 T}{\partial y^2} + \Lambda \left[D_B \frac{\partial C}{\partial y} \frac{\partial T}{\partial y} + \frac{D_T}{T_\infty} \left(\frac{\partial T}{\partial y} \right)^2 \right] - \frac{1}{(\rho c)_f} \frac{\partial q_r}{\partial y} \\ = \alpha T_f \frac{a}{\nu} \theta'' + \Lambda \left[D_B C_\infty T_f \frac{a}{\nu} \theta' \phi' + \frac{D_T}{T_\infty} a \frac{T_f^2}{\theta'^2} \nu \right] + \frac{1}{(\rho c)_f} \frac{16\sigma^* T_\infty^3 a \theta''}{3k^* \nu} \end{aligned} \quad (3.15)$$

Hence the dimensionless form of Eq. (3.3) becomes:

$$\begin{aligned} -T_f a f \theta' &= \alpha T_f \frac{a}{\nu} \theta'' + \Lambda \left[D_B C_\infty T_f \frac{a}{\nu} \theta' \phi' + \Lambda \frac{D_T}{T_\infty} a \frac{T_f^2}{\theta'^2} \nu \right] + \frac{1}{(\rho c)_f} \frac{16\sigma^* T_\infty^3 a \theta''}{3k^* \nu}, \\ -f \theta' &= \frac{\alpha}{\nu} \theta'' + \frac{(\rho c)_p}{(\rho c)_f} \frac{D_B}{\nu} C_\infty \theta' \phi' + \frac{(\rho c)_p}{(\rho c)_f} \frac{D_T T_f}{T_\infty \nu} \theta'^2 + \frac{4}{3} \frac{k}{(\rho c)_f \nu} \left(\frac{4\sigma^* T_\infty^3}{kk^*} \right) \theta'', \\ -f \theta' &= \frac{1}{Pr} \theta'' + Nb \theta' \phi' + Nt \theta'^2 + \frac{4}{3Pr} Nr \theta'', \\ -Pr f \theta' &= \theta'' + \frac{4}{3} Nr \theta'' + Pr [Nb \theta' \phi' + Nt \theta'^2] \end{aligned} \quad (3.16)$$

$$-Pr f \theta' = \left(1 + \frac{4}{3} Nr \right) \theta'' + Pr [Nb \theta' \phi' + Nt \theta'^2],$$

$$\left(1 + \frac{4}{3} Nr \right) \theta'' + Pr [f \theta' + Nb \theta' \phi' + Nt \theta'^2] = 0. \quad (3.17)$$

Next to transform Eq. (3.4) into the dimensionless form, we consider the following derivatives

- $u \frac{\partial C}{\partial x} + v \frac{\partial C}{\partial y} = D_B \left(\frac{\partial^2 C}{\partial y^2} \right) + \frac{D_T}{T_\infty} \left(\frac{\partial^2 T}{\partial y^2} \right)$
- $\frac{\partial C}{\partial x} = 0$
- $\frac{\partial C}{\partial y} = \frac{a}{\nu} C_\infty \phi'$
- $\frac{\partial^2 C}{\partial y^2} = \frac{\partial}{\partial y} \left(C_\infty \phi' \frac{a}{\nu} \right)$
- $v = -\sqrt{av} f(\eta)$

Hence the dimensionless form of Eq. (3.4) becomes:

$$-afC_\infty\phi' = D_B C_\infty \phi'' \frac{a}{\nu} + \frac{D_T}{T_\infty} (T_f - T_\infty) \theta'' \frac{a}{\nu},$$

$$-\frac{(\rho c)_p}{(\rho c)_f} f C_\infty \phi' = \frac{(\rho c)_p}{(\rho c)_f} D_B C_\infty \phi'' \frac{1}{\nu} + \frac{(\rho c)_p}{(\rho c)_f} \frac{D_T}{T_\infty} (T_f - T_\infty) \theta'' \frac{a}{\nu},$$

$$\frac{-D_B}{\nu} \frac{(\rho c)_p}{(\rho c)_f} C_\infty f \phi' \frac{\nu}{\alpha} = Nb \phi'' + Nt \theta'',$$

$$-NbPrLe f \phi' = Nb \phi'' + Nt \theta'',$$

$$-PrLe f \phi' = \phi'' + \frac{Nt}{Nb} \theta'',$$

$$\phi'' + \frac{Nt}{Nb} \theta'' + PrLe f \phi' = 0. \tag{3.18}$$

After using similarity transformation the equations take the form

$$\left. \begin{aligned} (1-n)f''' + ff'' - f'^2 - Mf' + nWef'''f'' &= 0, \\ \left(1 + \frac{4}{3}N_r\right)\theta'' + Pr\left(f\theta' + Nb\phi'\theta' + Nt\theta'^2\right) &= 0, \\ \phi'' + PrLef\phi' + \frac{Nt}{Nb}\theta'' &= 0. \end{aligned} \right\} \quad (3.19)$$

The associated boundary condition are transformed as follows:

- $u = u_w + U_{slip} \Rightarrow axf'(\eta) = ax + A\frac{a^{\frac{3}{2}}x(f''(\eta))}{\sqrt{\nu}} + B\frac{a^2x(f'''(\eta))}{\sqrt{\nu}}$
- $f'(\eta) = 1 + A\sqrt{\frac{a}{\nu}}(f''(\eta)) + B\frac{a}{\nu}(f'''(\eta)) \quad \left(\because \eta = \sqrt{\frac{a}{\nu}}y\right)$
 $= 1 + \gamma(f''(\eta)) + \delta(f'''(\eta))$
- $v = 0 \Rightarrow \sqrt{a\nu}f(\eta) \Rightarrow \sqrt{a\nu} \neq 0$
- $f(\eta) = 0 \Rightarrow f(0) = 0$
- $-k\frac{\partial T}{\partial y} = h_f(T_f - T)$
 $-k(T_f - T_\infty)\theta'\sqrt{\frac{a}{\nu}} = h_f((T_f - T_\infty) + \theta((T_f - T_\infty)))$
 $-k\theta'\sqrt{\frac{a}{\nu}} = h_f(1 + \theta)$
- $\theta' = -\frac{h_f}{k}\sqrt{\frac{\nu}{a}}(1 + \theta)$
 $\theta'(0) = Bi(\theta(0) - 1) \quad \left(\because Bi = \frac{h_f}{k}\sqrt{\frac{\nu}{a}}\right)$
- $D_B\frac{\partial C}{\partial y} + \frac{D_B}{T_\infty} = 0$
 $\Rightarrow D_B C_\infty \phi' \sqrt{\frac{a}{\nu}} + \frac{D_B}{T_\infty}(T_f - T_\infty)\theta' \sqrt{\frac{a}{\nu}}$
 $\Rightarrow \frac{(\rho c_p)}{(\rho c)_f} \sqrt{\frac{a}{\nu}} D_B C_\infty \phi' \sqrt{\frac{a}{\nu}} + \frac{(\rho c)_p}{(\rho c)_f} \sqrt{\frac{a}{\nu}} + D_B(T_f - T_\infty)\theta' \sqrt{\frac{a}{\nu}}$
 $\Rightarrow \frac{(\rho c_p)}{(\rho c)_f} D_B C_\infty \phi' + \frac{(\rho c)_p}{(\rho c)_f} + D_B(T_f - T_\infty)\theta'$

$$\Rightarrow Nb\phi'(0) + Nt\theta'(0)$$

Hence the dimensionless form of the boundary conditions become:

$$\left. \begin{aligned} f(0) = 0, \quad f'(0) = 1 + \gamma f''(0) + \delta f'''(0), \\ \theta'(0) = Bi(\theta(0) - 1), \quad Nb\phi'(0) + Nt\theta'(0) = 0, \\ f'(\infty) \rightarrow 0, \quad \theta(\infty) \rightarrow 0, \quad \phi(\infty) \rightarrow 0, \quad \text{as } \eta \rightarrow \infty. \end{aligned} \right\} \text{ at } \eta = 0, \quad (3.20)$$

The physical parameters appeared in Eq. (3.19) and Eq. (3.20), We represents the Weissenberg number, Bi the Biot number, Pr is the representation of the Prandtl number, Nr represents the thermal radiation parameter, M denotes the magnetic parameter, Le denotes the Lewis number, Nt stands for thermophoresis parameter, slip velocity of first order is denoted by γ , δ is the slip velocity of second order and Brownian motion parameter is denoted by Nb . These parameters are formulated as:

$$We = \frac{\sqrt{2}a^{\frac{2}{3}}x\Gamma}{\sqrt{\nu}}, \quad M = \frac{\sigma B_0^2}{\rho_f a}, \quad Bi = \frac{h_f}{k} \sqrt{\frac{\nu}{a}}, \quad Pr = \frac{\nu}{\alpha}, \quad Nr = \frac{4\sigma^* T_\infty^3}{\kappa^* k},$$

$$Nb = \frac{(\rho c)_p D_B (C_\infty)}{(\rho c)_f \nu}, \quad Le = \frac{\alpha}{D_B}, \quad Nt = \frac{(\rho c)_p D_T (T_f - T_\infty)}{(\rho c)_f \nu T_\infty}, \quad \gamma = A \sqrt{\frac{a}{\nu}}, \quad \delta = B \frac{a}{\nu}.$$

3.3 Physical Quantities of Interest

The mathematical expression of skin friction coefficient is defined below:

$$C_f = \frac{\tau_w}{\rho u_w^2}, \quad (3.21)$$

and mathematical expression for Nusselt number is:

$$Nu_x = \frac{xq_w}{k(T_f - T_\infty)}, \quad (3.22)$$

where τ_w stands for shear stress whereas q_w is representation of heat flux at the wall, given as:

$$\tau_w = \mu \left((1-n) \frac{\partial u}{\partial y} + \frac{n\Gamma}{\sqrt{2}} \left(\frac{\partial u}{\partial y} \right)^2 \right), \quad q_w = -k \left(1 + \frac{16\sigma^* T_\infty^3}{3\kappa^* k} \right) \frac{\partial T}{\partial y}. \quad (3.23)$$

Using the values of $\frac{\partial u}{\partial y} = \frac{a^{\frac{3}{2}} x f''(\eta)}{\sqrt{\nu}}$, we have

$$C_f = \frac{\nu \rho (1-n) \frac{a^{\frac{3}{2}} x f''(\eta)}{\sqrt{\nu}} + \frac{n \Gamma}{\sqrt{2}} \left(\frac{a^{\frac{3}{2}} x f''(\eta)}{\sqrt{\nu}} \right)^2}{\rho (ax)^2}$$

$$C_f = \frac{\nu a^{-\frac{1}{2}} (1-n)}{x \sqrt{\nu}} f''(\eta) + \frac{n \Gamma a}{\sqrt{2}} f''(\eta)^2 \quad \left(\because \mu = \nu \rho \right)$$

$$C_f = \sqrt{\frac{\nu}{a}} \frac{(1-n) f''(\eta)}{x} + \sqrt{\frac{a \nu}{a \nu}} \frac{x n \sqrt{2} \Gamma f''(\eta)^2}{2x}$$

$$C_f = \frac{(1-n) f''(\eta)}{\sqrt{Re_x}} + \frac{n}{2} f''(\eta)^2 \frac{a^{\frac{3}{2}} x \Gamma}{\sqrt{\nu} x} \sqrt{\frac{\nu}{a}}$$

$$C_f = \frac{(1-n) f''(\eta)}{\sqrt{Re_x}} + \frac{n}{2 \sqrt{Re_x}} f''(\eta)^2 We$$

$$C_f \sqrt{Re_x} = (1-n) f''(0) + \frac{n}{2} We f''(0)^2$$

$$Nu_x = \frac{x q_w}{k(T_f - T_\infty)}$$

$$Nu_x = \frac{x \left(-k \left(1 + \frac{16 \sigma^* T_\infty^3}{3k^* k} \right) \frac{\partial T}{\partial y} \right)}{k(T_f - T_\infty)}$$

Similarly utilizing the values of $\frac{\partial T}{\partial y} = \theta'(T_f - T_\infty) \sqrt{\frac{a}{\nu}}$

$$Nu_x = \frac{-x \left(1 + \frac{16 \sigma^* T_\infty^3}{3k^* k} \right) \theta'(T_f - T_\infty) \sqrt{\frac{a}{\nu}}}{(T_f - T_\infty)}$$

$$Nu_x = -x \sqrt{\frac{a}{\nu}} \left(1 + \frac{4}{3} Nr \right) \theta'$$

$$\frac{Nu_x}{\sqrt{Re_x}} = \left(1 + \frac{4}{3} Nr \right) \theta'(0)$$

Hence the dimensionless form of C_f and Nu_x is given as:

$$\left. \begin{aligned} C_f \sqrt{Re_x} &= \left((1-n) + \frac{n}{2} We f''(0) \right) f''(0), \\ Nu_x Re_x^{-1/2} &= - \left(1 + \frac{4}{3} N_r \right) \theta'(0) \end{aligned} \right\} \quad (3.24)$$

where $Re_x = \frac{ax^2}{\nu}$ denotes the local Reynolds number.

3.4 Numerical Technique

The system of higher order ODEs is converted into first order ODEs. The prescribed boundary conditions are also converted into first order system of ordinary differential equations (ODEs). The first order system of ordinary differential equations including the related boundary conditions is solved numerically by the use of MATLAB built-in function `bvp4c`.

$$\left. \begin{aligned} f''' &= \frac{1}{1-n+nWe f''} \left[f'^2 + Mf' - ff'' \right], \\ \theta'' &= -\frac{3Pr}{3+4N_r} \left[f\theta' + Nb\phi'\theta' + Nt\theta'^2 \right], \\ \phi'' &= -PrLe f\phi' - \frac{Nt}{Nb} \theta'' \end{aligned} \right\} \quad (3.25)$$

along with the boundary condition:

$$\left. \begin{aligned} f(0) = 0, \quad f'(0) = 1 + \gamma f''(0) + \delta f'''(0), \quad \theta'(0) = Bi(\theta(0) - 1), \\ Nb\phi'(0) + Nt\theta'(0) = 0, \quad \text{as } \eta = 0, \\ f'(\infty) \rightarrow 0, \quad \theta(\infty) \rightarrow 0, \quad \phi(\infty) \rightarrow 0, \quad \text{as } \eta \rightarrow \infty \end{aligned} \right\}. \quad (3.26)$$

By using the following notations:

$$\begin{aligned} f &= y_1, \quad f' = y_2, \quad f'' = y_3, \quad f''' = y'_3, \\ \theta &= y_4, \quad \theta' = y_5, \quad \theta'' = y'_5, \\ \phi &= y_6, \quad \phi' = y_7, \quad \phi'' = y'_7. \end{aligned} \quad (3.27)$$

The system of first order ODEs are given as:

$$\begin{aligned}
y_1' &= y_2 \\
y_2' &= y_3 \\
y_3' &= \frac{1}{(1-n) + nWe y_3} \left[y_2^2 + My_2 - y_1 y_3 \right] \\
y_4' &= y_5 \\
y_5' &= \frac{-3Pr}{3 + 4N_r} \left[y_1 y_5 + Nby_7 y_5 + Nry_5^2 \right] \\
y_6' &= y_7 \\
y_7' &= -PrLe y_1 y_7 - \frac{Nt}{Nb} y_5'
\end{aligned} \tag{3.28}$$

along with the initial condition which are

$$\left. \begin{aligned}
y_1(0) = 0, \quad y_2(0) = 1 + \gamma y_3(0), \quad y_5(0) = Bi(y_4(0) - 1), \\
Nby_7(0) + Nty_5(0) = 0 \quad \text{as } \eta \rightarrow 0.
\end{aligned} \right\} \tag{3.29}$$

In Table 3.1, comparison of the local skin friction coefficient by use of various values of parameter M is displayed. Furthermore, the obtained numerical results are compared with Ibrahim [34] and achieved a good agreement.

3.5 Result and Discussion

The main purpose of this part is to analyze the velocity, temperature, and concentration profiles. The computations are taken out for the influence of various natural parameters like, the Prandtl number, the power-law index, the brownian motion parameter, the Weissenberg number, the thermal radiation parameter, the Biot number, first order slip parameter and second order slip parameter on the Nusselt number and skin friction coefficient. Table 3.2 is prepared to study the impact of various parameters on the coefficient of skin friction. It is observed that for enhancing the Power-law index and the magnetic parameter the skin friction is reduced. For the increasing values of the Weissenberg number We , first order slip Parameter γ , and second order slip parameter δ the skin friction coefficient

Table 3.1: Numerical results of skin friction for increasing values of M with $We = \delta = n = \gamma = 0$.

M	Ibrahim [34]	Present
0.0	1.0000	1.0001
0.25	1.1180	1.1180
1	1.4142	1.4142
5	2.4495	2.4494
10	3.3166	3.3166
50	7.1414	7.1414
100	10.0499	10.0499
500	22.3830	22.3830
1000	31.6386	31.6386

is declined. To analyze the impact of Power-law index (n) on velocity, energy and concentration fields. Figures 3.2 and 3.3 are sketched. It is noticed that for enhancing the value of physical parameter called Power-law index, the velocity field is decreased while temperature profile is increased. Physically, the parameter n , defines the shear thickening behaviour of fluid. Therefore, as magnitude of n is increased more resistance is provided to the fluid due to this reason velocity is reduced. Figure 3.4 shows that, for some growing values of n , concentration profile is increasing function of parameter n . Figure 3.5 and Figure 3.6 demonstrate the impact of Weissenberg number on velocity distribution and temperature distribution. The Weissenberg number is defined as, the ratio of relaxation time and the time-scale of the fluid flow. By enhancing the values of the Weissenberg number, momentum boundary layer and the velocity distribution is reduced. For enhancing values of We the relaxation time increases, that permit more resistance to the flow, because of this reason the temperature field and thickness of related boundary layer is increased. Figure 3.7 reflects the influence of first order slip on velocity field, by increasing the value of first order slip parameter, velocity

Table 3.2: Numerical results of skin friction $-f''(0)$ for gradually increasing values of physical parameters.

We	n	M	γ	δ	$f''(0)$	
					Ibrahim [34]	present
0.1	0.3	0.2	1	-1	0.3317	0.3317
					0.3312	0.3312
					0.3308	0.3308
	0.1				0.3287	0.3286
	0.2				0.3300	0.3301
	0.3				0.3308	0.3305
		0.1			0.3288	0.3288
		0.2			0.3308	0.3301
		0.5			0.3307	0.3306
		0.2			0.3308	0.3308
			2		0.2477	0.2477
			3		0.1978	0.1978
			2		0.2477	0.2477
				-2	0.2053	0.2053
				-3	0.1770	0.1770

field started decreasing and hydrodynamic boundary layer is thinner. From Figure 3.8 and Figure 3.9 it is observed that temperature and concentration field is increasing function of γ . Figure 3.10 shows the impact of slip parameter of second order on velocity field. By enhancing the value of slip parameter δ , velocity field started decreasing and hydrodynamic boundary layer is thinner. Figure 3.11 and 3.12 demonstrate the effect of second order slip parameter on temperature field and concentration profile, it is clear that slip parameter is enhancing function of temperature and concentration profile. Figure 3.13 shows the impact of thermal Radiation parameter Nr , here it is shown that temperature field is increased as magnitude of Nr is increased. This is because of the fact that an increment in the values of Nr tend to reduce the thickness of the momentum boundary surface and increase the rate of heat transfer. Figure 3.14 explained the effect of the Biot number Bi on temperature field. By increasing the value of dimensionless parameter Bi , the temperature at the surface is increased which increases the thermal boundary layer. Physically, the Biot number is basically the ratio between resistance of the heat transfer in the body to the resistance at body surface. This is

because of the fact that convective heat exchange along the surface will enhance the momentum boundary layer. Impact of the Prandtl number for the variation of temperature distribution is visualized in Figure 3.15, this figure gives the evident that fluid with increasing values of the Prandtl number represent weak energy diffusion so for higher values of the Prandtl number results a strong reduction in temperature field.

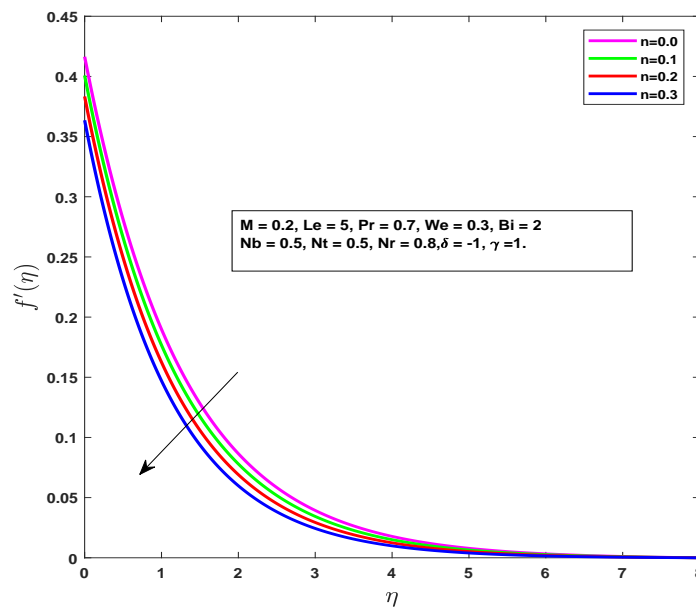


Figure 3.2: Effect of n on $f'(\eta)$.

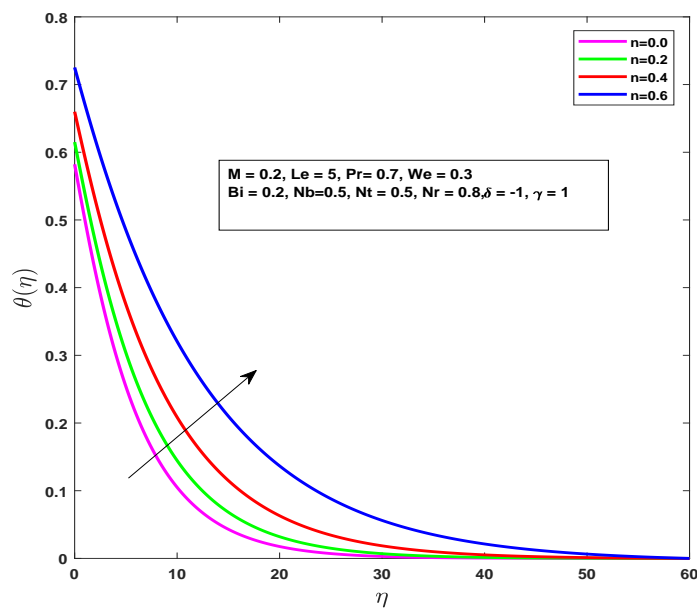


Figure 3.3: Effect of n on $\theta(\eta)$.

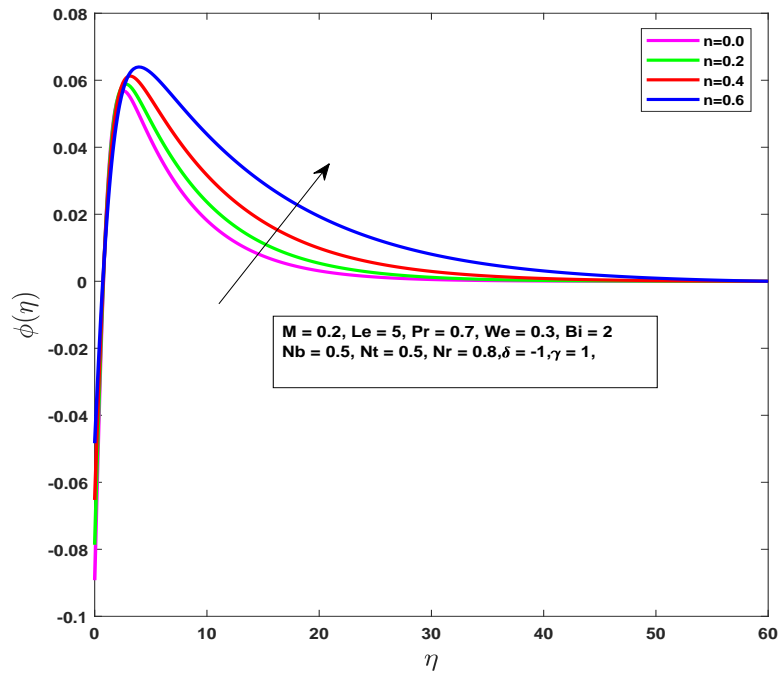


Figure 3.4: Effect of n on $\phi(\eta)$.

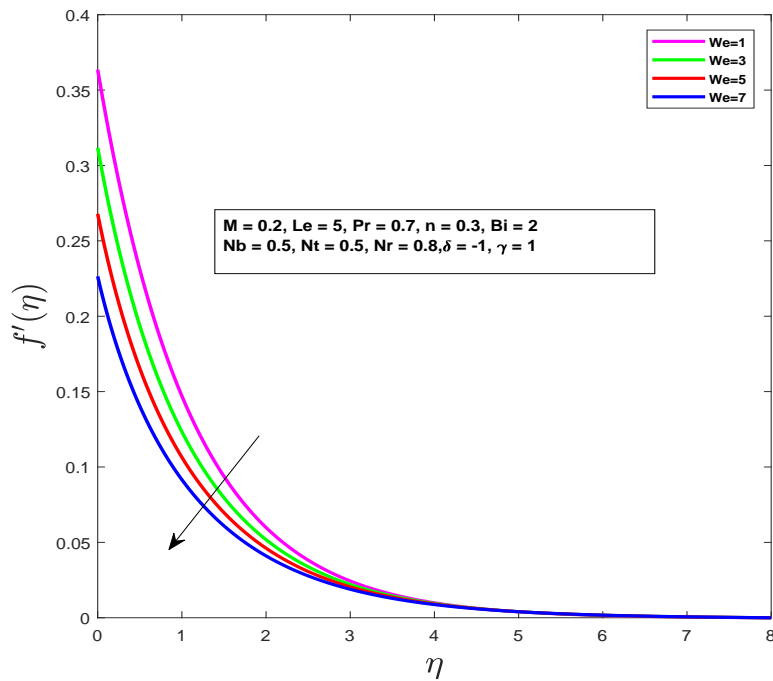


Figure 3.5: Effect of We on $f'(\eta)$.

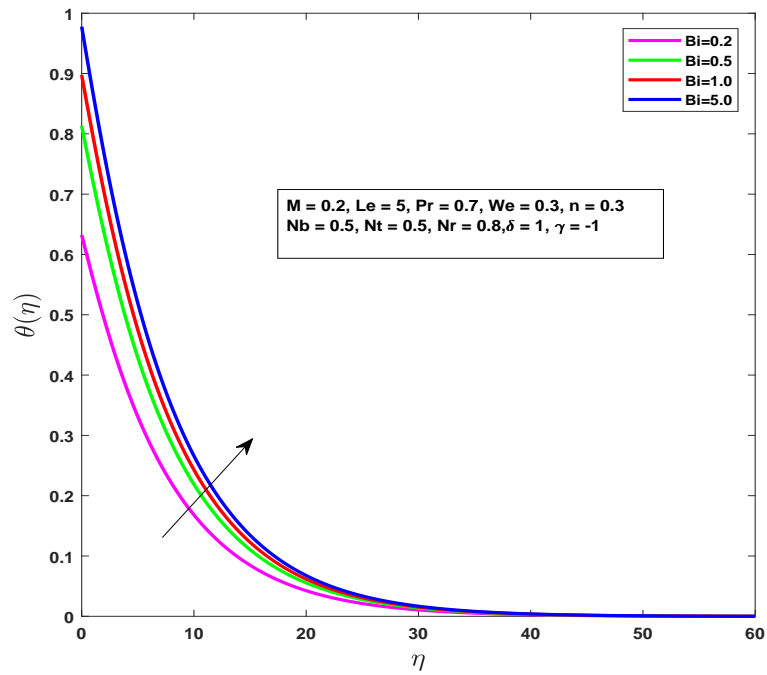


Figure 3.6: Effect of Bi on $\theta(\eta)$.

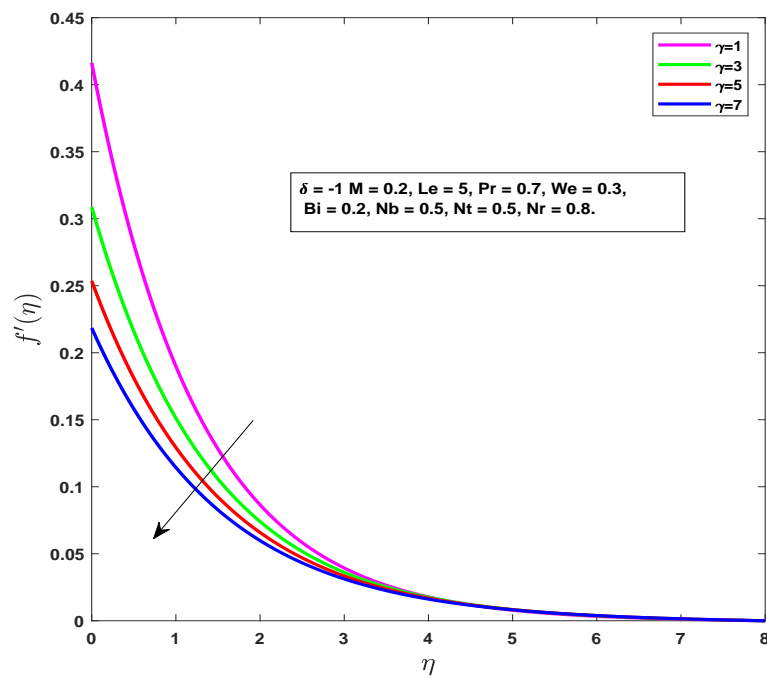


Figure 3.7: Effect of γ on $f'(\eta)$.

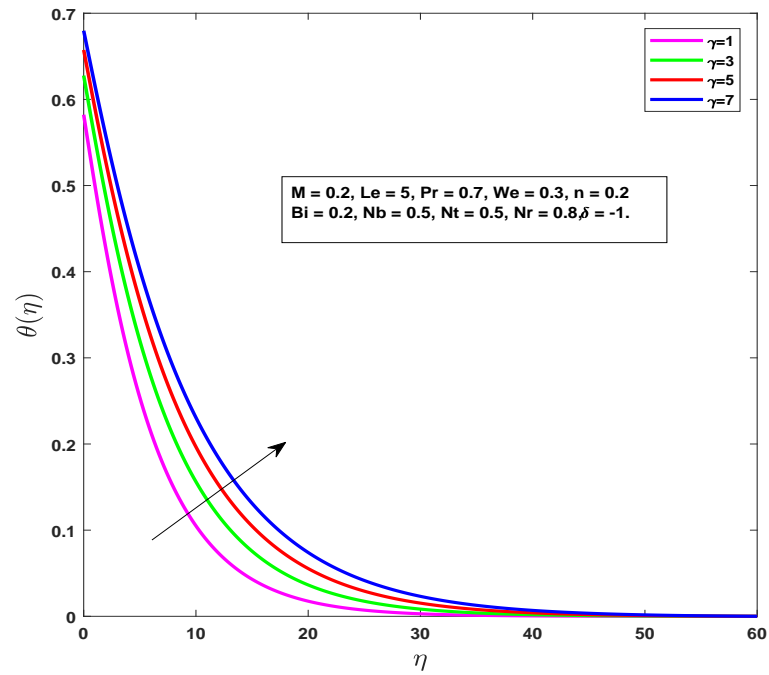


Figure 3.8: Effect of γ on $\theta(\eta)$.

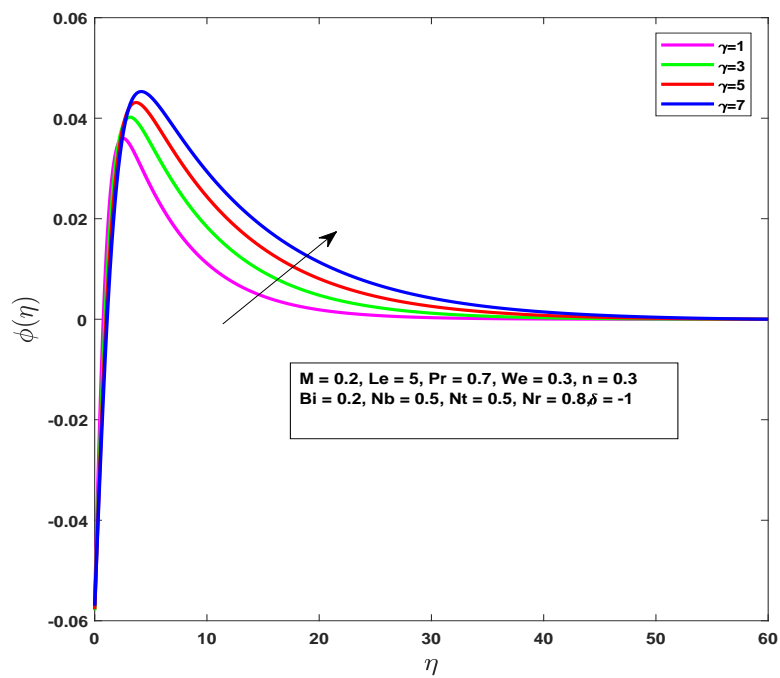


Figure 3.9: Effect of γ on $\phi(\eta)$.

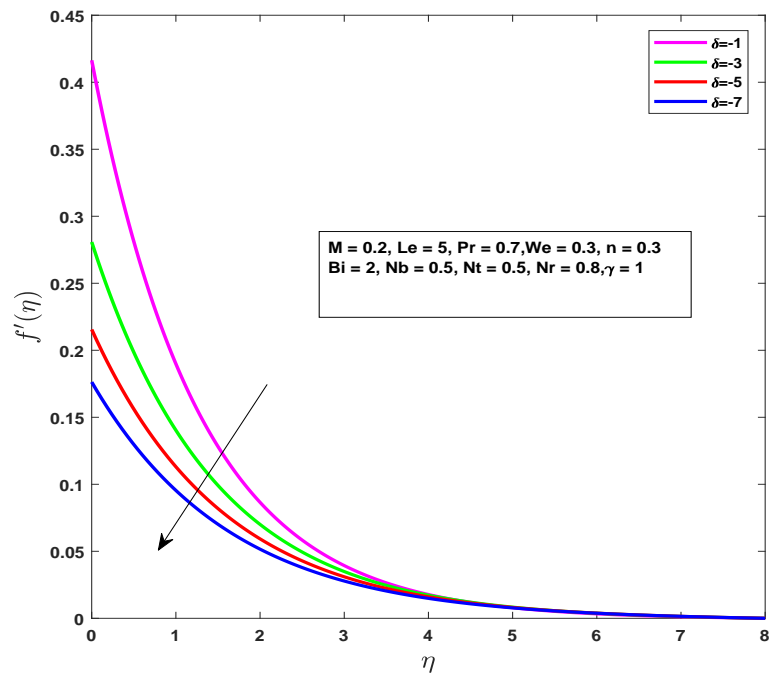


Figure 3.10: Effect of δ on $f'(\eta)$.

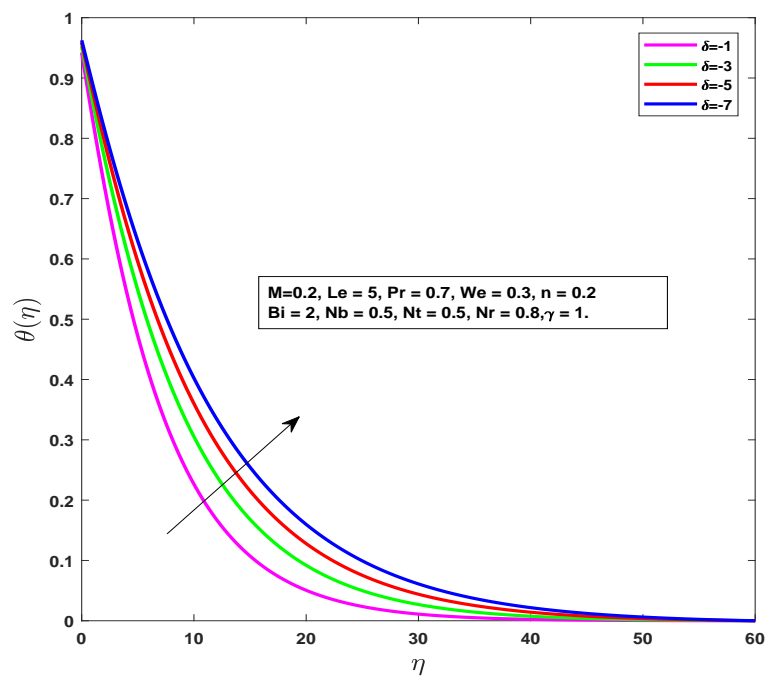


Figure 3.11: Effect of δ on $\theta(\eta)$.

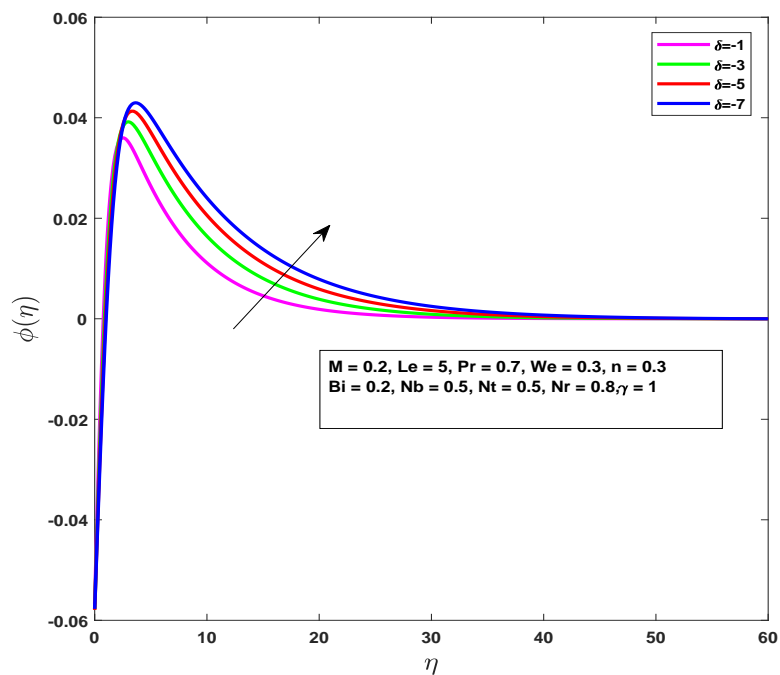


Figure 3.12: Effect of δ on $\phi(\eta)$.

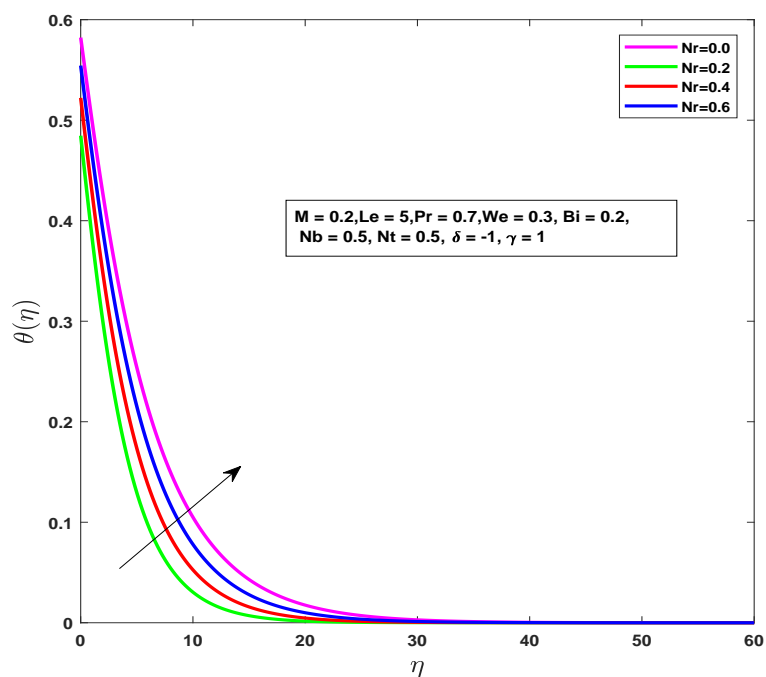


Figure 3.13: Effect of Nr on $\theta(\eta)$.

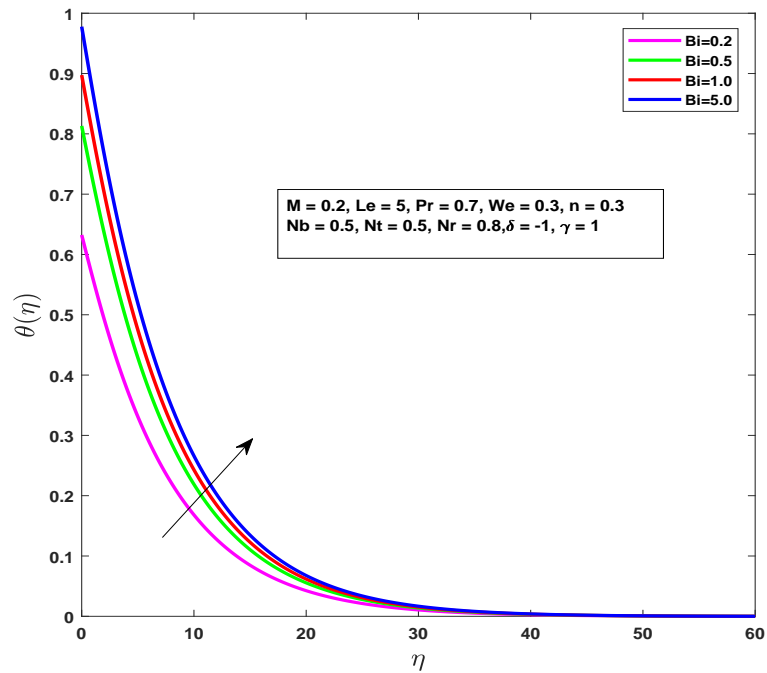


Figure 3.14: Effect of Bi on $\theta(\eta)$.

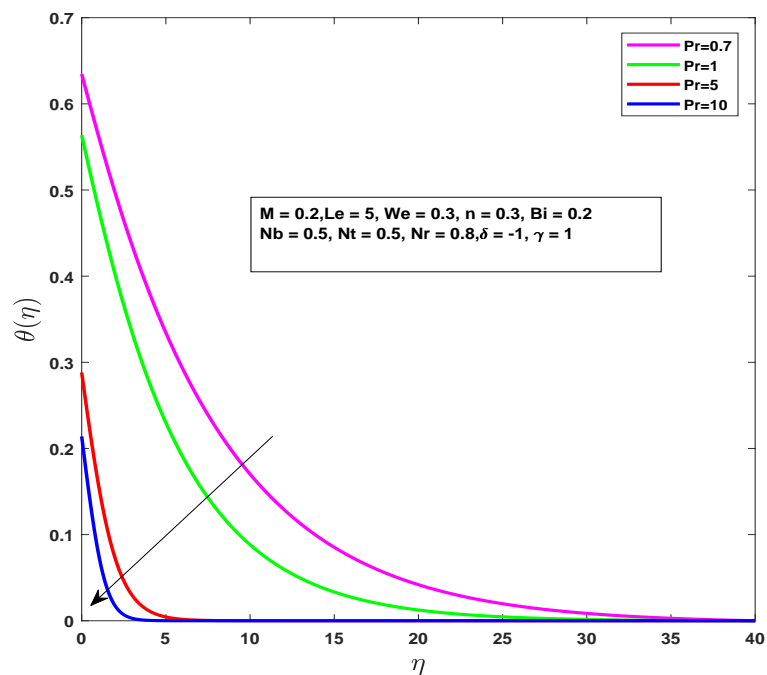


Figure 3.15: Effect of Pr on $\theta(\eta)$.

Chapter 4

Impact of Chemical Reaction and Joule Heating on MHD Nanofluid

The main purpose of this section is to examine the magneto-hydrodynamic tangent hyperbolic fluid flow along a sheet under the effect of Joule heating and chemical reaction. Nonlinear PDEs are converted in to a system of ODEs by using an appropriate similarity transformation. We have achieved the numerical solution of the system of ODEs by using the technique namely the shooting technique along with Runge-Kutta method of order four. The results for different parameters for velocity, energy and concentration profile are deliberated through graphical and tabular form.

4.1 Mathematical Modeling

The Laminar, two-dimensional and steady MHD tangent hyperbolic nanofluid taken along a stretching surface, is considered. It has been assumed that the fluid under investigation is taken as viscous and incompressible. In addition to the assumption as described in Section 3.2, the Joule heating and chemical reaction impact has also been incorporated.

Under the above constraint the related equations are given as:

$$\frac{\partial u}{\partial x} + \frac{\partial v}{\partial y} = 0, \quad (4.1)$$

$$u \frac{\partial u}{\partial x} + v \frac{\partial u}{\partial y} = \nu(1-n) \frac{\partial^2 u}{\partial y^2} + \sqrt{2\nu n} \Gamma \left(\frac{\partial u}{\partial y} \right) \frac{\partial^2 u}{\partial y^2} - \frac{\sigma B_0^2 u}{\rho_f}, \quad (4.2)$$

$$u \frac{\partial T}{\partial x} + v \frac{\partial T}{\partial y} = \alpha \left(\frac{\partial^2 T}{\partial y^2} \right) + \Lambda \left[D_B \left(\frac{\partial C}{\partial y} \right) \left(\frac{\partial T}{\partial y} \right) + \frac{D_T}{T_\infty} \left(\frac{\partial T}{\partial y} \right)^2 \right] - \frac{1}{(\rho c)_f} \frac{\partial q_r}{\partial y} + \frac{\sigma B_0^2 u^2}{\rho_f}, \quad (4.3)$$

$$u \frac{\partial C}{\partial x} + v \frac{\partial C}{\partial y} = D_B \frac{\partial^2 C}{\partial y^2} + \frac{D_T}{T_\infty} \left(\frac{\partial^2 T}{\partial y^2} \right) - K_r(C - C_\infty). \quad (4.4)$$

The related boundary conditions are as follows [34]:

$$\left. \begin{aligned} u = u_w, \quad -k \frac{\partial T}{\partial y} = h_f(T_f - T), \\ v = 0, \quad D_B \frac{\partial C}{\partial y} + \frac{D_B}{T_\infty} \frac{\partial T}{\partial y} = 0, \\ U \rightarrow U_\infty, \quad v = 0, \quad T \rightarrow T_\infty, \quad C \rightarrow C_\infty \quad \text{as } y \rightarrow \infty. \end{aligned} \right\} \text{ at } y = 0 \quad (4.5)$$

Here ρ stands for density of nanoparticles, u and v define velocity components, D_T is thermophoresis diffusion coefficient, k represents the thermal conductivity, D_B the Brownian diffusion coefficient, T_∞ denotes the ambient temperature, $\Lambda = \frac{(C_p)_p}{(C_p)_f}$, $(C_p)_p$ is the fluid's specific heat capacity of nanoparticles, $(C_p)_f$ the heat capacity of the fluid and Γ represents the time constant.

4.2 Similarity Transformation

In this section similar to Chapter3, we transform the system of PDEs along with boundary condition into a dimensionless form by using appropriate similarity transformations. The similarity transformation used are as follows:

$$\psi = \sqrt{a\nu x} f(\eta), \quad \eta = \sqrt{\frac{a}{\nu}} y, \quad \phi(\eta) = \frac{C - C_\infty}{C_\infty}, \quad \theta(\eta) = \frac{T - T_\infty}{T_f - T_\infty}. \quad (4.6)$$

The velocity components in terms of the stream functions are given as,

$$u = \frac{\partial \psi}{\partial y}, \quad v = -\frac{\partial \psi}{\partial x}. \quad (4.7)$$

As a result Eq. (4.1) is satisfied identically and equations (4.2)-(4.4) take the form

$$\left. \begin{aligned} (1-n)f''' + ff'' - f'^2 - Mf' + nWe f''' f'' &= 0, \\ \left(1 + \epsilon\theta + \frac{4}{3}Nr\right)\theta'' + Pr \left[f\theta' + Nb\phi'\theta' + Nt\theta'^2 + MEcf'^2\right] &= 0, \\ \phi'' + \frac{Nt}{Nb}\theta'' + fSc\phi' + Sck_1\phi &= 0. \end{aligned} \right\} \quad (4.8)$$

The transformed boundary conditions are:

$$\left. \begin{aligned} f(0) = 0, \quad f'(0) = 1, \\ \theta'(0) = Bi(\theta(0) - 1), \quad Nb\phi'(0) + Nt\theta'(0) = 0, \\ f'(\infty) \rightarrow 0, \quad \theta(\infty) \rightarrow 0, \quad \phi(\infty) \rightarrow 0, \quad \text{as } \eta \rightarrow \infty. \end{aligned} \right\} \text{ at } \eta = 0, \quad (4.9)$$

In Eq. (4.8) and Eq. (4.9), We represents the Weissenberg number, Bi the Biot number, Pr represents the Prandtl number, Brownian motion parameter is denoted by Nb , M denotes the magnetic parameter, Le stands for the Lewis number, Nt is thermophoresis parameter, Ec represents the Eckert number and radiation parameter is denoted by Nr . These parameters are formulated as:

$$Nt = \frac{(\rho c)_p D_T (T_f - T_\infty)}{(\rho c)_f \nu T_\infty}, \quad Bi = \frac{h_f}{k} \sqrt{\frac{\nu}{a}}, \quad Pr = \frac{\nu}{\alpha}, \quad Nr = \frac{4\sigma^* T_\infty^3}{\kappa^* k}, \quad M = \frac{\sigma B_0^2}{\rho_f a},$$

$$Sc = \frac{\nu}{D_B}, \quad Nb = \frac{(\rho c)_p D_B (C_\infty)}{(\rho c)_f \nu}, \quad Nt = \frac{(\rho c)_p D_T (T_f - T_\infty)}{(\rho c)_f \nu T_\infty}, \quad We = \frac{\sqrt{2} a^{\frac{2}{3}} x \Gamma}{\sqrt{\nu}}.$$

4.2.1 Physical Quantities of Interest

The dimensional form of skin friction coefficient C_f is:

$$C_f = \frac{\tau_w}{\rho u_w^2}, \quad (4.10)$$

and the dimensional form of Nusselt number Nu_x is

$$Nu_x = \frac{xq_w}{k(T_f - T_\infty)}, \quad (4.11)$$

where wall shear stress is represented by τ_w whereas the wall heat flux is denoted by q_w both are represented as:

$$\tau_w = \mu \left((1-n) \frac{\partial u}{\partial y} + \frac{n\Gamma}{\sqrt{2}} \left(\frac{\partial u}{\partial y} \right)^2 \right), \quad q_w = -k \left(1 + \frac{16\sigma^* T_\infty^3}{3k^* k} \right) \frac{\partial T}{\partial y}. \quad (4.12)$$

The local skin friction coefficient and the local Nusselt number in non-dimensional form which is:

$$\left. \begin{aligned} C_f \sqrt{Re_x} &= \left((1-n) + \frac{n}{2} We f''(0) \right) f''(0), \\ Nu_x Re_x^{-1/2} &= - \left(1 + \frac{4}{3} N_r \right) \theta'(0). \end{aligned} \right\} \quad (4.13)$$

where $Re_x = \frac{ax^2}{\nu}$ is defined the local Reynolds number.

4.3 Numerical Solution

The solution of the system of equation (4.8) along with boundary conditions (4.9) can achieved by use of shooting technique.

In order to solve the system of equation with shooting technique we convert the ODEs into first order ODEs. Equation (4.8) can be rewritten as,

$$\left. \begin{aligned} f''' &= \frac{1}{(1-n) + nWe f''} [f'^2 + Mf' - ff''], \\ \theta'' &= - \frac{Pr}{\left(1 + \epsilon\theta + \frac{4}{3} N_r \right)} \left[f\theta' + Nb\phi'\theta' + Nt\theta'^2 + MEcf'^2 \right], \\ \phi'' &= \frac{Nt}{Nb} \theta'' - fSc\phi' - Sck_1\phi. \end{aligned} \right\} \quad (4.14)$$

Boundary condition in dimensionless shape is:

$$\left. \begin{aligned} y_1(\eta) = 0, \quad y_2(\eta) = 1, \quad y_5(\eta) = Bi(y_4(\eta) - 1), \\ Nby_7(\eta) + Nty_5(\eta) = 0, \quad \text{as } \eta = 0, \\ y_2(\infty) \rightarrow 0, \quad y_4(\infty) \rightarrow 0, \quad y_6(\infty) \rightarrow 0, \quad \text{as } \eta \rightarrow \infty \end{aligned} \right\}. \quad (4.15)$$

By using such notations which are:

$$\left. \begin{aligned} f = y_1, \quad f' = y_2, \quad f'' = y_3, \quad f''' = y_3', \\ \theta = y_4, \quad \theta' = y_5, \quad \theta'' = y_5', \\ \phi = y_6, \quad \phi' = y_7, \quad \phi'' = y_7', \end{aligned} \right\}. \quad (4.16)$$

The system of first order ODEs are given as:

$$\left. \begin{aligned} y_1' &= y_2 \\ y_2' &= y_3 \\ y_3' &= \frac{y_2^2 + My_2 - y_1y_3}{(1-n) + nWe y_3} \\ y_4' &= y_5 \\ y_5' &= \frac{-Pr(y_1y_5 + Nby_7y_5 + Nty_5^2 + 2MEcy_2^2)}{\left(1 + \epsilon\theta + \frac{4}{3}Nr\right)} \\ y_6' &= y_7 \\ y_7' &= -Scy_1y_7 - Sck_1y_7 + \frac{Nt}{Nb}y_5' \end{aligned} \right\}. \quad (4.17)$$

along with boundary conditions which are given below,

$$\left. \begin{aligned} y_1(0) = 0, \quad y_2(0) = 1, \quad y_3(0) = l, \quad y_4(0) = m \\ y_5(0) = Bi(t-1), \quad y_6(0) = n, \quad y_7(0) = -\frac{Nt}{Nb}Bi(t-1). \end{aligned} \right\} \quad (4.18)$$

To solve the boundary value problem (4.3)-(4.3) with the help of shooting technique seven initial conditions are needed. So, we initialize $y_3(0) = L$, $y_4(0) = m$ and $y_6(0) = n$ in such a way that three unknown boundary conditions are almost

satisfied for growing values of η i.e $\eta \rightarrow \infty$. Newton method is used to modify initial guesses l , m and n until the desired approximation meet. For iterative process we have defined the criteria where process is stopped that is given as

$$\max(|y_2(\eta_{max}) - 0|, |y_5(\eta_{max}) - 0|, |y_7(\eta_{max}) - 0|) < \zeta,$$

where ζ is a real number which is very small. For all the computation in the remaining part of this dissertation, ζ will be same as 10^{-5} .

4.4 Result and Discussion

The demonstration of this part is to analyze numerical results represented in the form of graphs and tables. Impact of different parameters such as the Prandtl number (Pr), the Biot number (Bi), the Brownian motion parameter (Nb), the power-law index, the Weissenberg number (We), radiation parameter (Nr) and thermophoresis parameter Nt on temperature distribution, velocity distribution and concentration profile are shown. We will see that as we are increasing the values of Magnetic parameter (M), Prandtl number (Pr) and power-law index (n) results a decline in the Nusselt number while an increment is shown in skin friction coefficient.

Impact of Magnetic Parameter M

Impact of magnetic parameter on velocity distribution and temperature distribution is presented in Figure 4.1 and Figure 4.2. Figure 4.1 is drawn to visualize that the velocity distribution is reduced for the enhancing values of the M where the temperature profile is enhanced as evident from Figure 4.2.

Physically, increase in magnetic field increases the Lorentz forces which is retarding force because of this reason fluid motion is declined and energy field is enhanced.

Table 4.1: numerical results of skin friction $-f''(0)$ and Nusselt number $-\theta'(0)$ for distinct values of Ec, Sc, Nb and Nt .

M	n	We	Bi	Pr	$-f''(0)$		$-\theta'(0)$	
					shooting	bvp4c	shooting	bvp4c
0.2	0.3	0.3	0.2	2	1.3924	1.3924	0.1414	0.1414
					1.4535	1.4535	0.1407	0.1407
					1.5126	1.5126	0.1407	0.1407
	0.2				1.2650	1.2650	0.1424	0.1424
	0.4				1.5853	1.5853	0.1400	0.1400
		0.2			1.3620	1.3620	0.1415	0.1415
		0.5			1.4664	1.4664	0.1411	0.1411
			1.5		1.3924	1.3924	0.3546	0.3546
			2		1.3924	1.3924	0.1284	0.1284
				0.7	1.3924	1.3924	0.1237	0.1237
				1	1.3924	1.3924	0.1284	0.1284

Impact of Power-law Index n

The effect of the parameter power-law index for velocity field and temperature field is presented in Figure 4.3 and Figure 4.4. From figures 4.3 and 4.4 it is clear that an increment in power-law index n , velocity field is decreased. The dimensionless parameter n defines the shear thinning behaviour of fluid, therefore by increasing the magnitude of n , more resistance is provided to fluid velocity due to this reason the flow of fluid is decreased.

Impact of Weissenberg Number We

The dimensionless parameter We is the ratio of fluid relaxation, due to increasing the values of Weissenberg number (We) the fluid's relaxation time increases, which

allow extra resistance to the flow. Figure 4.5 demonstrate the impact of the Weissenberg number. From figure it is clear that, for enhancing values of the Weissenberg number We , temperature profile increases which causes the effect of the thickness of momentum boundary layer.

Impact of Prandtl Number Pr

Figure 4.6 is drawn to analyze the impact of the Prandtl number (Pr) on temperature field. It is observed that for increasing value of the Prandtl number temperature field decreases, this is due to the fact that an decrement is seen in the rate of heat transfer for enhancing values of Pr . The impact of the Prandtl number on concentration profile is portrays in Figure 4.7. It portrays that an increment in (Pr) results a reduction in concentration field.

Impact of Thermophoresis Parameter Nt

Figure 4.8 and Figure 4.9 are presented to visualize the effect of thermophoresis parameter on the temperature and concentration profile. In figures, it is observed that temperature profile and concentration profile show an increment for growing values of dimensionless parameter Nt . Physically, heated particles comes away from high temperature as compared to low-temperature so the temperature of fluid increases.

Impact of Radiation Parameter Nr

Impact of Radiation parameter is shown in Figure 4.10. It is seen that for gradually enhancing values of Nr energy profile also increased. Due to increase in thermal Radiation parameter more heat to fluid produces that enhance the energy filed

and momentum boundary layer. Figure 4.11 also represents that concentration profile is increased for increasing values of radiation parameter.

Impact of Biot Number Bi

Figure 4.12 is presented to visualize the effect of the Bi on temperature distribution. This figure defines that temperature profile enhances as the Biot number Bi is increased gradually. Physically, the Biot number defines the ratio between resistance rate of heat transfer inside the body to the resistance at the body surface. The reason behind is that convective heat exchange at the surface will raise the boundary layer thickness therefore the nanofluid with convective boundary condition is more effective model as compared to the constant surface temperature state.

Impact of Small Parameter ϵ

To illustrate the impact of small parameter ϵ which is associated with the variable thermal conductivity on the temperature field, Figure 4.14 represents that by enhancing the values of small parameter ϵ temperature profile also enhanced.

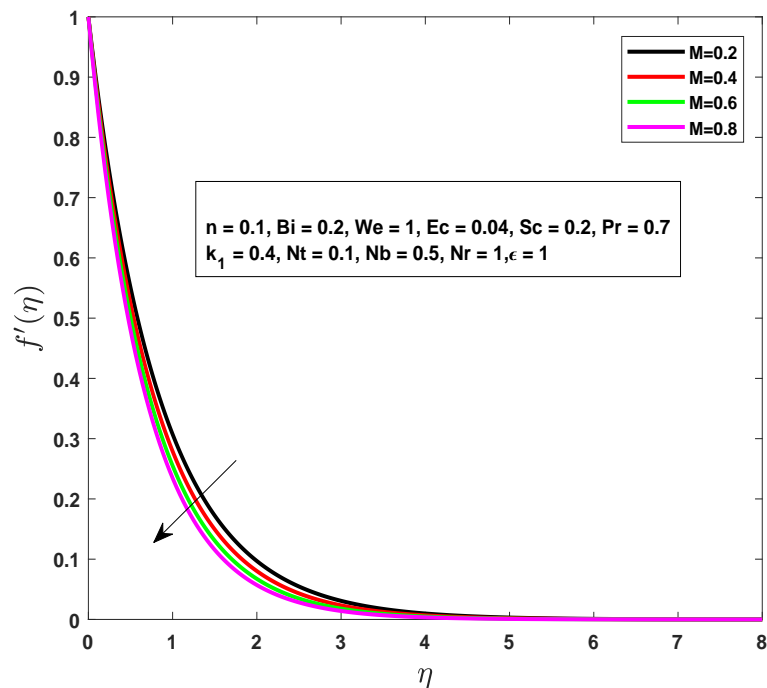


Figure 4.1: Effect of M on $f'(\eta)$.

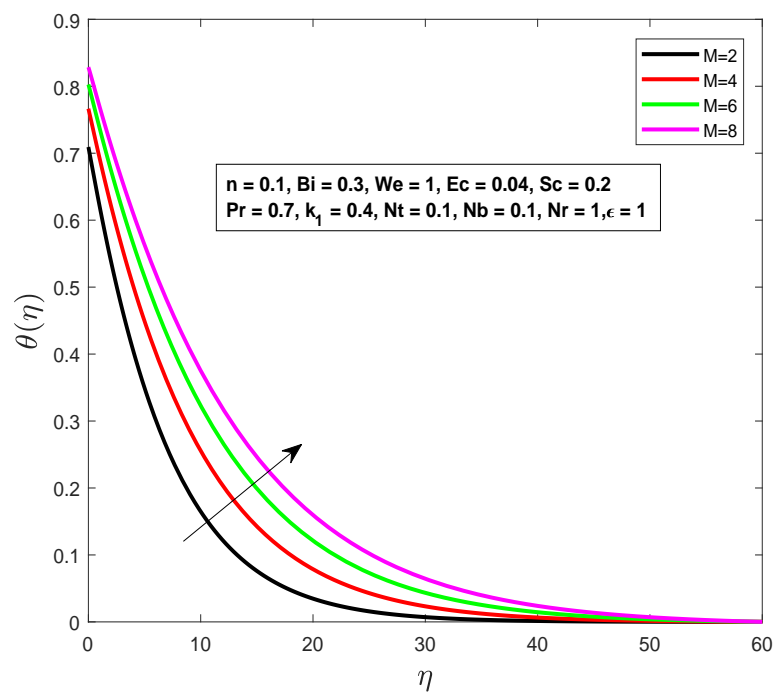
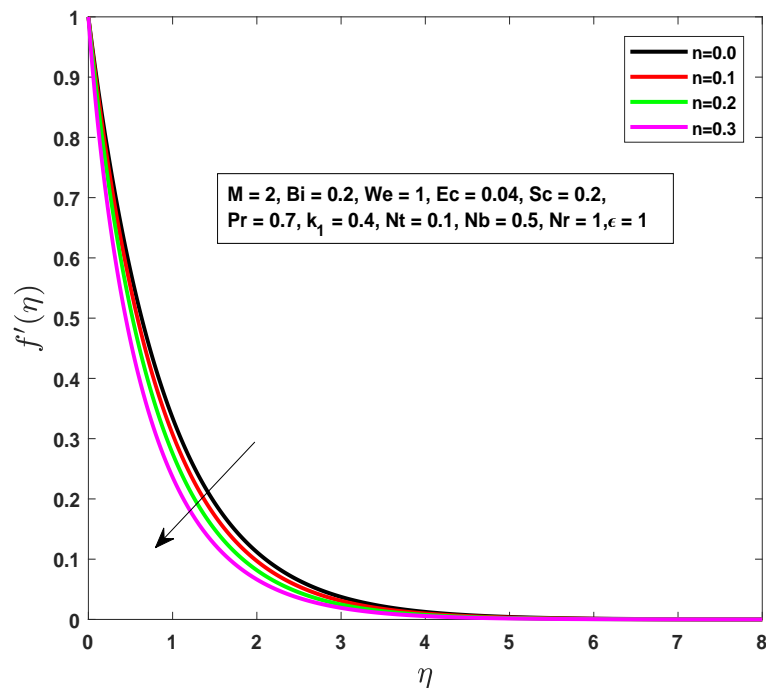
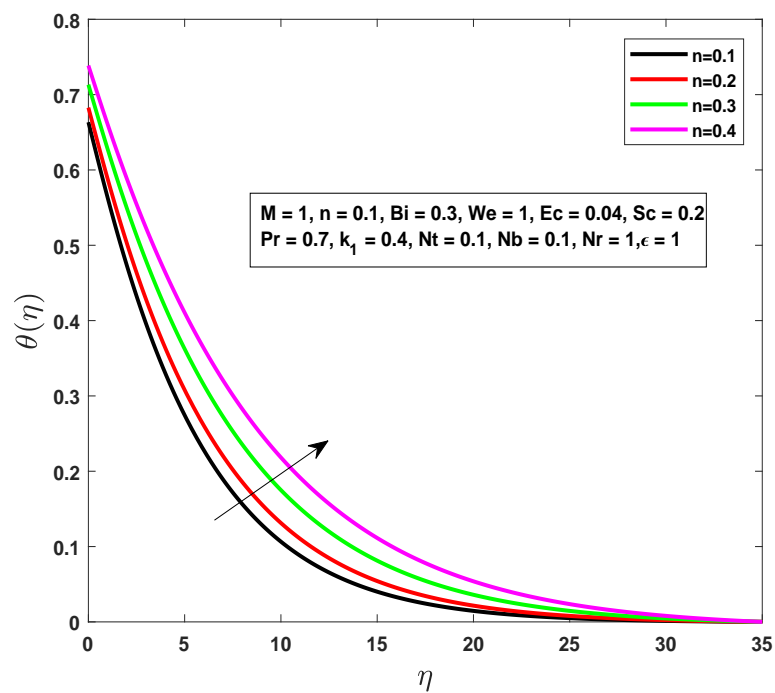


Figure 4.2: Effect of M on $\theta(\eta)$.

Figure 4.3: Effect of n on $f'(\eta)$.Figure 4.4: Effect of n on $\theta(\eta)$.

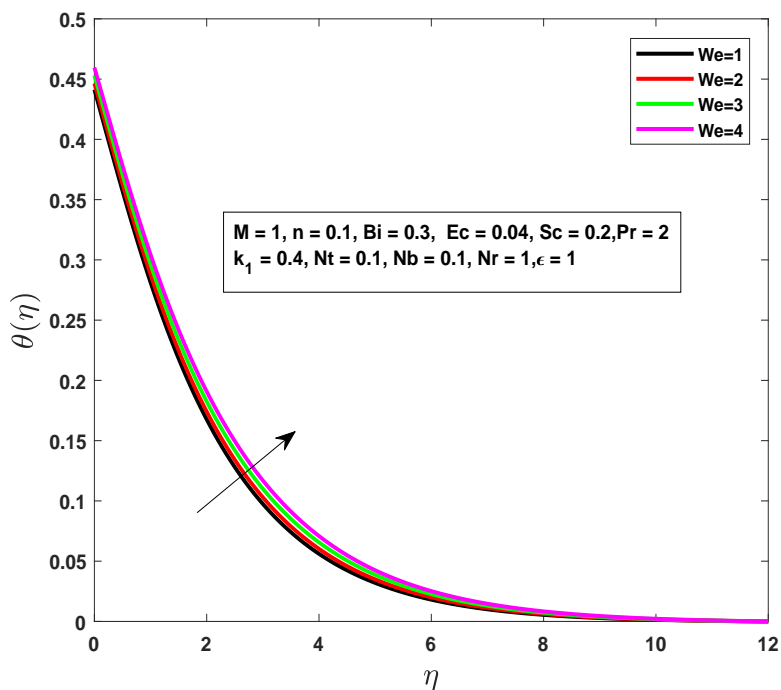


Figure 4.5: Effect of We on $\theta(\eta)$.

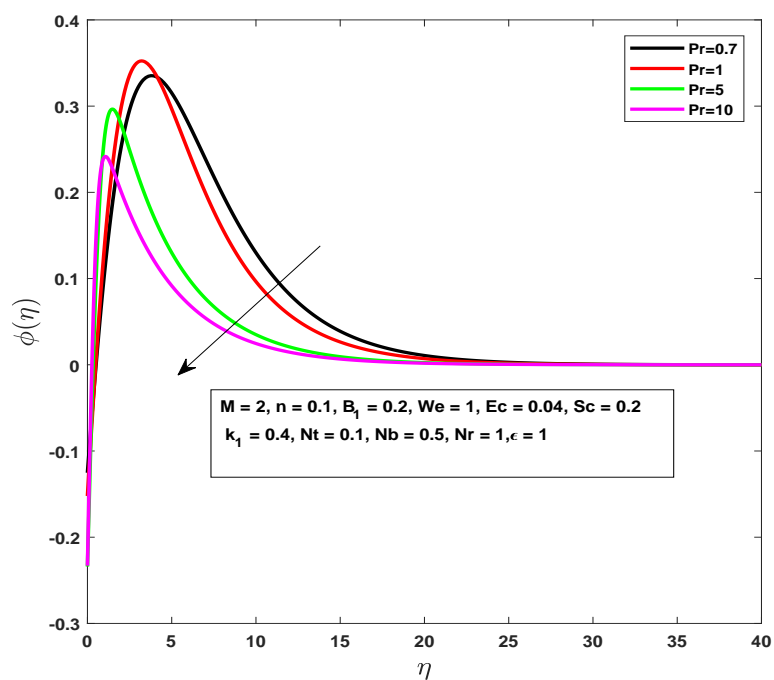


Figure 4.6: Effect of Pr on $\theta(\eta)$.

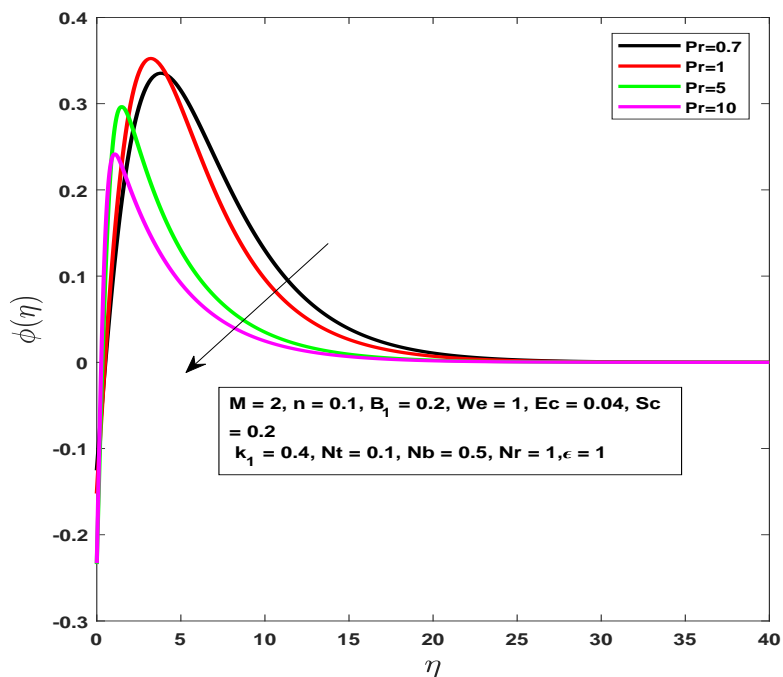


Figure 4.7: Effect of Pr on $\phi(\eta)$.

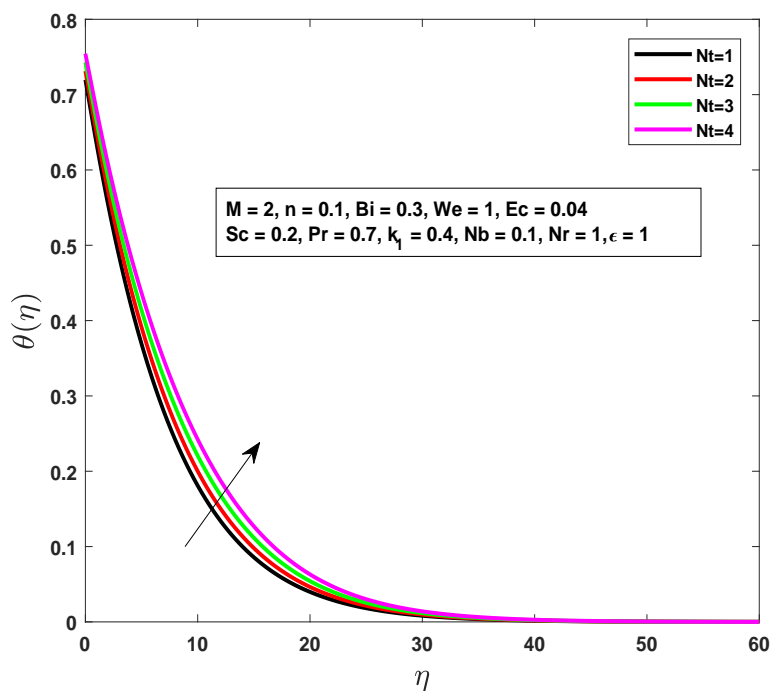


Figure 4.8: Effect of Nt on $\theta(\eta)$.

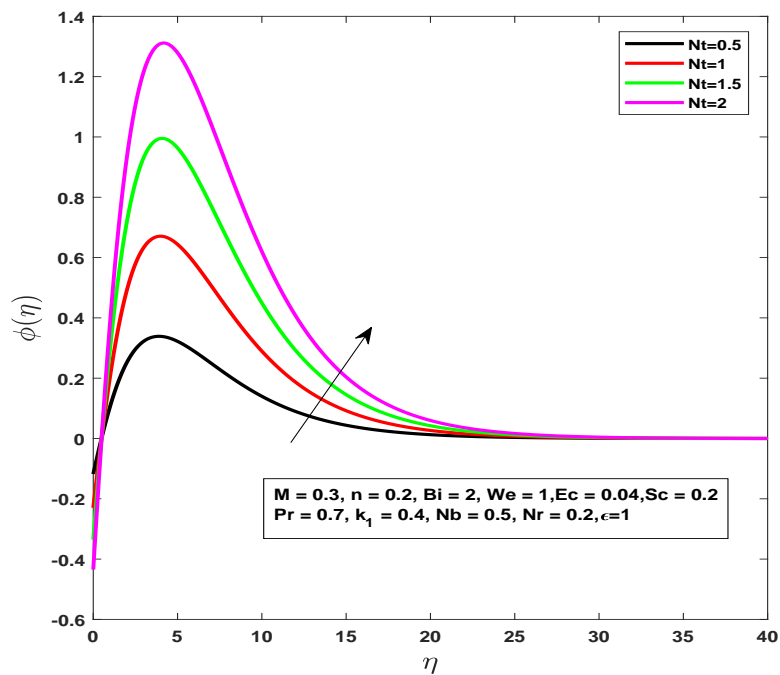


Figure 4.9: Effect of Nt on $\phi(\eta)$.

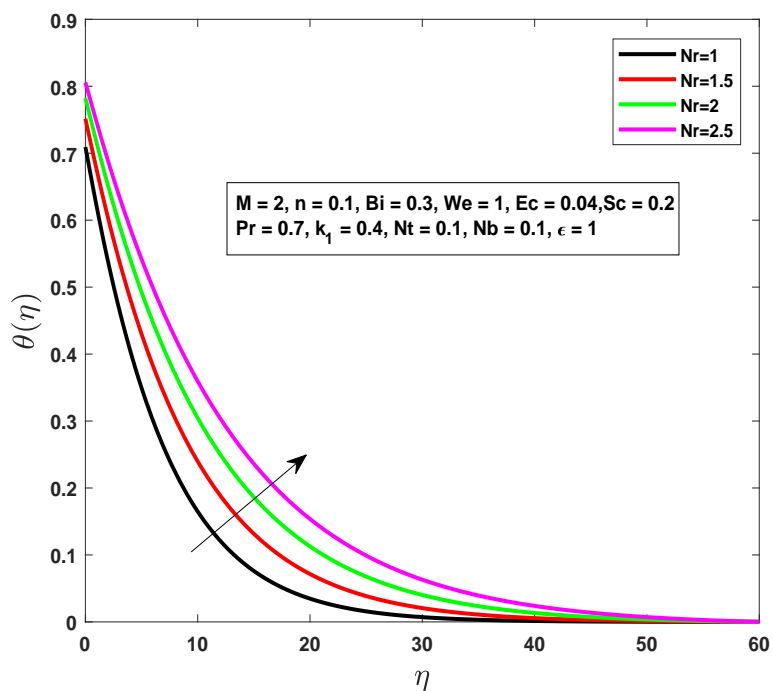
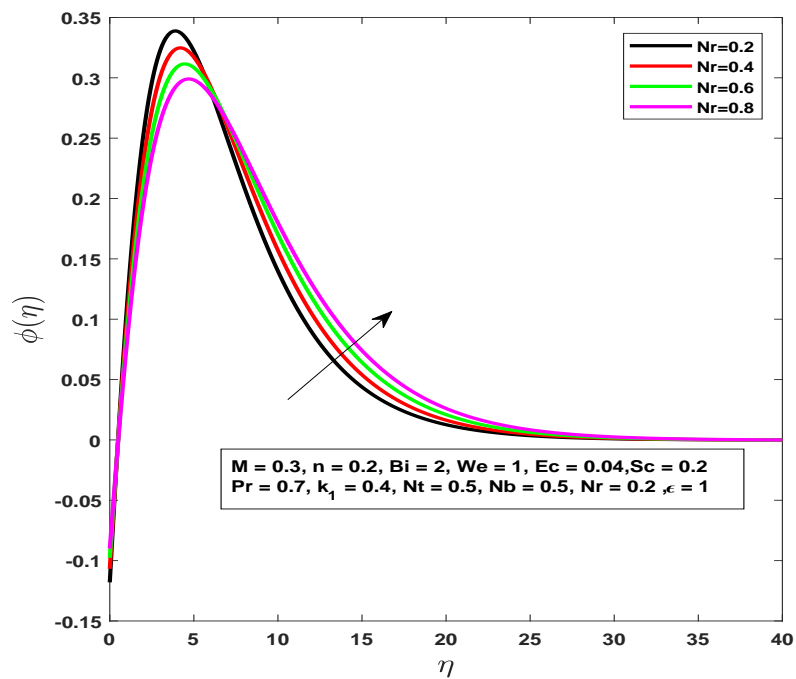
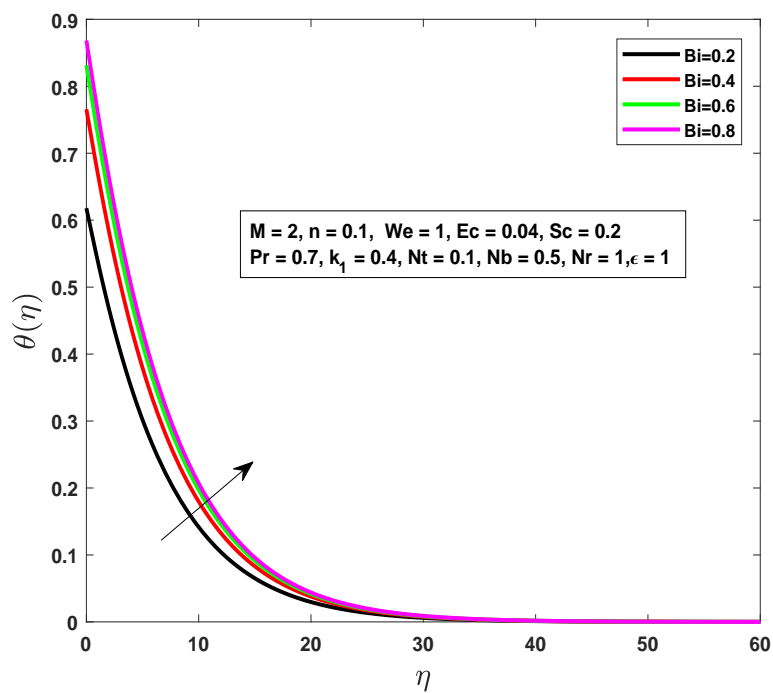


Figure 4.10: Effect of Nr on $\theta(\eta)$.

Figure 4.11: Effect of Nr on $\phi(\eta)$.Figure 4.12: Effect of Bi on $\theta(\eta)$.

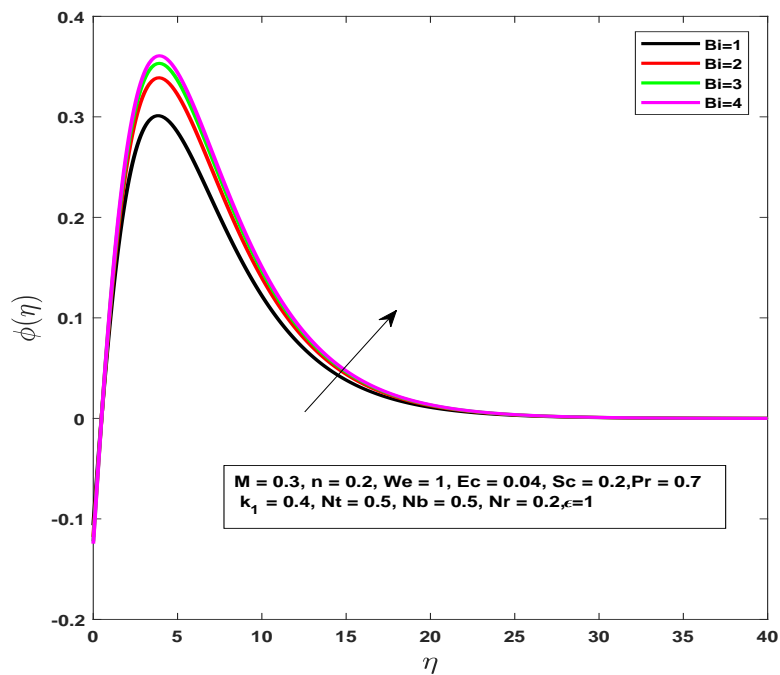


Figure 4.13: Effect of Bi on $\phi(\eta)$.

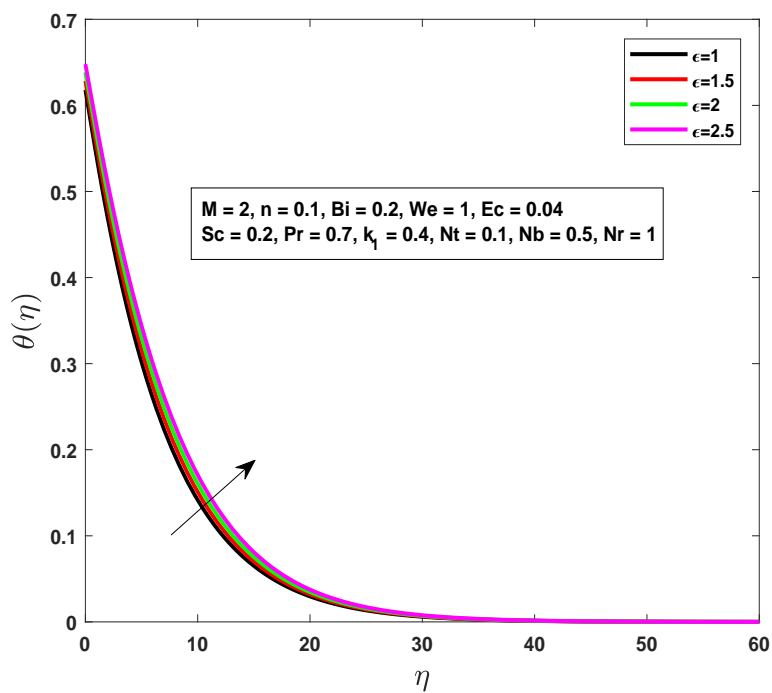


Figure 4.14: Effect of ϵ on $\theta(\eta)$.

Chapter 5

Conclusion

In this thesis, we reviewed the work of Ibrahim [35] and analyse the effect of chemical reaction and Joule heating. First of all momentum equations, energy equations and concentration equations converted into the ODEs by using an appropriate transformation called similarity transformation. By using the shooting technique, numerical solution has been found for these modeled ODEs. Using different values of governing physical parameters we found results in the form of tables and graphs for velocity profile, temperature profile and concentration profile. Concluding all arguments and results we summarized our findings as follows:

- An increment in the values of the magnetic parameter and power-law index, energy profile is reduced while temperature profile is enhanced.
- For enhancing values of the Weissenberg number, thickness of momentum boundary layer enhances .
- Decrement in temperature profile and concentration profile is observed for increasing values of the prandtl number.
- The Nusselt number increases for increasing values of the thermophoresis parameter Nt , radiation parameter Nr and the Biot number Bi .
- It is reported that for enhancing values of the radiation parameter Nr , thermophoresis parameter Nt , and the Biot number Bi , concentration profile also enhanced.

Bibliography

- [1] T. Salahuddin, M. Y. Malik, A. Hussain, M. Awais, I. Khan, and M. Khan., “Analysis of tangent hyperbolic nanofluid impinging on a stretching cylinder near the stagnation point,” *Results in physics*, vol. 7, pp. 426–434, 2017.
- [2] B. C. Sakiadis., “Boundary-layer behavior on continuous solid surfaces,” *AIChE journal*, vol. 7, pp. 467–472, 1961.
- [3] L. J. Crane., “Flow past a stretching plate,” *Journal of Applied Mathematics and Physics*, vol. 21, pp. 645–647, 1970.
- [4] B. S. Dandapat and A. S. Gupta., “Flow and heat transfer in a viscoelastic fluid over a stretching sheet,” *International Journal of Non-Linear Mechanics*, vol. 24, pp. 215–219, 1989.
- [5] B. M. Genick., *Basics of fluid mechanics*. Potto Project, 2013, vol. 3, pp. 1–65.
- [6] L. Zehng, J. Niu, and L. Ma., “Dual solutions for flow and radiative heat transfer of a micropolar fluid over stretching/shrinking sheet,” *International Journal of Heat and Mass Transfer*, vol. 55, pp. 7577–7586, 2012.
- [7] B. J. Gireesha, A. J. Chamkha, S. Manjunatha, and C. S. Bagewadi., “Mixed convective flow of a dusty fluid over a vertical stretching sheet with nonuniform heat source/sink and radiation,” *International Journal of Numerical Methods for Heat & Fluid Flow*, vol. 23, pp. 598–612, 2013.
- [8] S. A. Shehzad, Z. Abdullah, F. M. Abbasi, T. Hayat, and A. Alsaedi., “Magnetic field effect in three-dimensional flow of an Oldroyd-B nanofluid over a

- radiative surface,” *Journal of Magnetism and Magnetic Materials*, vol. 399, pp. 97–108, 2016.
- [9] H. Alfvén., “Existence of electromagnetic-hydrodynamic waves,” *Nature*, vol. 150, p. 405, 1942.
- [10] M. M. Rashidi, N. V. Ganesh, A. K. Hakeem, and B. Ganga., “Buoyancy effect on MHD flow of nanofluid over a stretching sheet in the presence of thermal radiation,” *Journal of Molecular Liquids*, vol. 198, pp. 234–238, 2014.
- [11] N. Hari, S. Sivasankaran, M. Bhuvanewari, and Z. Siri., “Effects of chemical reaction on MHD mixed convection stagnation point flow toward a vertical plate in a porous medium with radiation and heat generation,” *Journal of Physics: Conference Series*, vol. 662, pp. 012–014, 2015.
- [12] C. Zhang, L. Zheng, X. Zhang, and G. Chen., “MHD flow and radiation heat transfer of nanofluids in porous media with variable surface heat flux and chemical reaction,” *Applied Mathematical Modelling*, vol. 39, pp. 165–181, 2015.
- [13] S. M. Ibrahim and K. Suneetha., “Heat source and chemical effects on MHD convection flow embedded in a porous medium with sores, viscous and Joules dissipation,” *Ain Shams Engineering Journal*, vol. 7, pp. 811–818, 2016.
- [14] M. Bilal, S. Hussain, and M. Sagheer., “Boundary layer flow of magneto-micropolar nanofluid flow with Hall and ion-slip effects using variable thermal diffusivity,” *Bulletin of the Polish Academy of Sciences Technical Sciences*, vol. 65, pp. 383–390, 2017.
- [15] T. Hayat, M. Waqas, and M. I. K. A. Alsaedi., “Impacts of constructive and destructive chemical reactions in magnetohydrodynamic (MHD) flow of Jeffrey liquid due to nonlinear radially stretched surface,” *Journal of Molecular Liquids*, vol. 225, pp. 302–310, 2017.

- [16] S. M. Atif, S. Hussain, and M. Sagheer., “Numerical study of MHD micropolar Carreau nanofluid in the presence of induced magnetic field,” *AIP Advances*, vol. 8, pp. 035–219, 2018.
- [17] S. U. S. Choi and J. A. Eastman., “Enhancing thermal conductivity of fluids with nanoparticles,” *ASME-Publications-Fed*, vol. 231, pp. 99–106, 1995.
- [18] S. U. S. Choi, Z. G. Zhang, W. Y. a. F. E. Lockwood, and E. A. Grulke., “Anomalous thermal conductivity enhancement in nanotube suspensions,” *Applied physics letters*, vol. 79, pp. 2252–2254, 2001.
- [19] K. Khanafer, K. Vafai, and M. Lightstone., “Buoyancy-driven heat transfer enhancement in a two-dimensional enclosure utilizing nanofluids,” *International Journal of Heat and Mass Transfer*, vol. 46, pp. 3639–3653, 2003.
- [20] M. Izadi, A. Behzadmehr, and D. J. Vahida., “Numerical study of developing laminar forced convection of a nanofluid in an annulus,” *International Journal of Thermal Sciences*, vol. 48, pp. 2119–2129, 2009.
- [21] K. V. Wong and O. D. Leon., “Applications of nanofluids: current and future,” *Advances in mechanical engineering*, vol. 2, pp. 519–659, 2010.
- [22] M. K. Nayak, N. S. Akbar, V. S. Pandey, Z. H. Khan, and D. Tripathi., “3D free convective MHD flow of nanofluid over permeable linear stretching sheet with thermal radiation,” *Powder Technology*, vol. 315, pp. 205–215, 2017.
- [23] K. G. Kumar, B. J. Gireesha, M. R. Krishnamurthy, and N. G. Rudraswamy., “An unsteady squeezed flow of a tangent hyperbolic fluid over a sensor surface in the presence of variable thermal conductivity,” *Results in Physics*, vol. 7, pp. 3031–3036, 2017.
- [24] T. Hayat, M. Waqas, A. Alsaedi, G. Bashir, and F. Alzahrani., “Magneto-hydrodynamic (MHD) stretched flow of tangent hyperbolic nanoliquid with variable thickness,” *Journal of Molecular Liquids*, vol. 229, pp. 178–184, 2017.
- [25] K. U. Rehman, A. A. Malik, M. Y. Malik, and N. U. Saba., “Mutual effects of thermal radiations and thermal stratification on tangent hyperbolic fluid

- flow yields by both cylindrical and flat surfaces,” *Case studies in thermal engineering*, vol. 10, pp. 244–254, 2017.
- [26] A. Shafiq, Z. Hammouch, and T. N. Sindhu., “Bioconvective MHD flow of tangent hyperbolic nanofluid with Newtonian heating,” *International Journal of Mechanical Sciences*, vol. 133, pp. 759–766, 2017.
- [27] M. Naseer, M. Yousaf, M. S. Nadeem, and A. Rehman., “The boundary layer flow of hyperbolic tangent fluid over a vertical exponentially stretching cylinder,” *Alexandria Engineering Journal*, vol. 53, pp. 747–750, 2014.
- [28] B. Prabhakar, S. Bandar, and R. U. Haq., “Impact of inclined Lorentz forces on tangent hyperbolic nanofluid flow with zero normal flux of nanoparticles at the stretching sheet,” *Neural Computing and Applications*, vol. 29, pp. 805–814, 2018.
- [29] R. Kandasamy, K. Periasamy, and K. K. S. Prabhu., “Effects of chemical reaction, heat and mass transfer along a wedge with heat source and concentration in the presence of suction or injection,” *International Journal of Heat and Mass Transfer*, vol. 48, pp. 1388–1394, 2005.
- [30] M. S. Alam, M. M. Rahman, and M. A. Sattar., “Effects of variable suction and thermophoresis on steady MHD combined free-forced convective heat and mass transfer flow over a semi-infinite permeable inclined plate in the presence of thermal radiation,” *International Journal of Thermal Sciences*, vol. 47, pp. 758–765, 2008.
- [31] Z. Abbas, M. Sheikh, and S. S. Motsa., “Numerical solution of binary chemical reaction on stagnation point flow of Casson fluid over a stretching/shrinking sheet with thermal radiation,” *Energy*, vol. 95, pp. 12–20, 2017.
- [32] A. K. Maleque., “Effects of binary chemical reaction and activation energy on MHD boundary layer heat and mass transfer flow with viscous dissipation and heat generation/absorption,” *ISRN Thermodynamics*, vol. 2013, pp. 284–637, 2013.

-
- [33] A. K. Malique., “Effects of exothermic/endothermic chemical reactions with arrhenius activation energy on MHD free convection and mass transfer flow in presence of thermal radiation,” *Journal of Thermodynamics*, vol. 2013, pp. 516–692, 2013.
- [34] W. Ibrahim., “Magnetohydrodynamics (MHD) flow of a tangent hyperbolic fluid with nanoparticles past a stretching sheet with second order slip and convective boundary condition,” *Results in Physics*, vol. 7, pp. 3723–3731, 2017.
- [35] R. K. Bansal., *A Text Book of Fluid Mechanics and Hydraulic Machines*. Laxmi publications, 1989, vol. 4, pp. 1–384.
- [36] J. Kunes., *Dimensionless physical quantities in science and engineering*. Elsevier, 2012, vol. 7, pp. 1–441.
- [37] A. Yunus., C. Cengel., and M. John., *Fluid mechanics fundamentals and applications*. Elsevier, 2012, vol. 3, pp. 1–817.
- [38] J. N. Reddy. and D. K. Gartling., *The finite element method in heat transfer and fluid dynamics*. CRC press, 2010, vol. 1, pp. 1–491.
- [39] M. Martini and P. Marcello., *Physics methods in archaeometry*. IOS press, 2004, vol. 3, pp. 1–734.
- [40] T. Y. Na., *Computational methods in engineering boundary value problems*. Academic press, 1980, vol. 145, pp. 1–306.